Root-Protograph-based BICM-ID: A Reliable and Efficient Transmission Solution for Block-Fading Channels

Yi Fang, Guohua Zhang, Guofa Cai, Francis C. M. Lau, Pingping Chen, and Guojun Han

Abstract

As a bandwidth-efficient technique, bit-interleaved coded modulation with iterative demapping and decoding (BICM-ID) has attracted much research attention in the field of wireless communication. In this paper, we put forth a joint design of root-protograph (RP) low-density parity-check (LDPC) codes and BICM-ID, referred to as *RP-based BICM-ID (RP-BICM-ID)*, over block-fading (BF) channels so as to boost the throughput under limited bandwidth. To preserve the full-diversity property of RP codes, we propose an efficient modulation strategy for the RP-BICM-ID system by taking the fading-block length into consideration. We also analyze the outage-probability limit of the RP-BICM-ID systems to establish the fundamental lower-limit on their word-error-rate (WER) performance. Moreover, we conceive a multi-level protograph extrinsic information transfer (ML-PEXIT) algorithm to derive the asymptotic WER and bit error rate (BER) of the RP-BICM-ID systems over BF channels. As a further insight, we develop a novel unequal-error-protection (UEP) bit-to-symbol (B2S) mapping scheme for the RP-BICM-ID systems, which gives rise to an additional performance improvement. Analyses and simulations show that the proposed RP-BICM-ID systems can not only realize desirable spectral efficiency, but also obtain near-outage-limit performance over BF channels. Therefore, the proposed RP-BICM-ID systems are very promising in achieving high-reliability and high-rate transmissions under slow-fading wireless-communication environments.

Block-fading (BF) channel, extrinsic information transfer (EXIT), protograph LDPC codes, spectral efficiency.

I. Introduction

The block-fading (BF) channel is of particular usefulness to describe wireless transmission scenarios with slowly varying fading [1]. In a BF channel, the fading gain keeps constant during each block within a codeword but varies randomly from block to block. This channel model is especially relevant in cellular networks, orthogonal-frequency-division-multiplexing (OFDM) systems, and free-space optical systems [2], [3]. In spite of its simplicity, the BF channel serves as one of the most important models for developing code-design criterion in wireless-communication systems. The code-design criteria developed in BF channels may also be applied to more practical channel models. Owing to the non-ergodic feature of BF channels, the classical capacity-approaching error-correction codes (ECCs), such as turbo code and low-density parity-check (LDPC) codes, are not able to approach the outage limits of BF channels [4].

Y. Fang and F. C. M. Lau are with the Hong Kong Polytechnic University, Hong Kong. G. Zhang is with China Academy of Space Technology (Xi'an), China. G. Cai and G. Han with the Guangdong University of Technology. P. Chen is with the Fuzhou University, China.

During the past two decades, a great deal of research effort has been devoted to analyzing and designing ECCs for BF channels. It has been demonstrated in [5] that the convolutional codes can realize full diversity in BF channels. However, such type of codes possesses word-error-rate (WER) performance sensitive to the codeword length, and thus is not suited to slow-fading transmission scenarios. To address the above issue, researchers have carried out an in-depth study of turbo codes and found that they can not only attain full diversity, but also achieve near-outage-limit performance after a careful design [6]. Moreover, a type of full-diversity LDPC codes (referred to as *root-LDPC codes*), which exhibits outage-limit-approaching performance under belief-propagation (BP) iterative decoding, has been constructed in [2]. Following the above work, several novel progressive-edge-growth (PEG) techniques have been conceived to construct the root-LDPC codes, referred to as *PEG-root-check LDPC codes*, over BF channels [7], [8]. Recently, the power allocation and decoding algorithms of root LDPC codes have also been discussed over BF channels [9], [10]. Compared with turbo codes, LDPC codes are amenable to relatively lower decoding complexity and thus have appeared to be a preferable choice for practical usage. Protograph LDPC codes, which preserve the advantages of conventional LDPC codes and enjoy the benefit of simple structure, have received growing interest in recent years [11], [12]. Inspired by the works of [2], [12], root-protograph (RP) codes have been conceived to acquire the desirable properties of both root-LDPC codes and protograph codes, e.g., full diversity, maximum rate, and easy design and implementation [13], [14].

In the BF channel, there is a tradeoff between diversity order and code rate. It has been proved in [1], [6] that the rate of any full-diversity ECC over a BF channel with L fading blocks is upper-bounded by $1/L$. As a result, the codes having full diversity over BF channels may suffer from relatively low transmission efficiency. As a bandwidth-efficient coded modulation scheme, bit-interleaved coded modulation (BICM) is capable of achieving both excellent error performance and high transmission rate (i.e., spectral efficiency) over fading channels with the help of an interleaver and high-order modulation [15]. Unfortunately, BICM is considered as a sub-optimal transmission scheme due to the independent demapping procedure. As an enhanced version of BICM with non-iterative receiver (BICM-NI), BICM with iterative demapping and decoding (BICM-ID), which substantially makes use of the a-priori information in demapping, can achieve identical performance as the optimal *coded modulation* [16]–[19].[1]

For the sake of realizing high-reliability and high-efficiency wireless communications, a significant amount of attention has been paid to investigating BICM-ID systems. In particular, a variety of ECCs have been exploited in BICM-ID systems so as to accomplish desirable performance in different channel conditions

[1]Although "BICM" is used to represent "BICM-NI" at its first occurrence, it will be used to represent "both BICM-NI and BICM-ID" from this point onwards.

[20]–[24]. As widely recognized, an interleaver is indispensable to guarantee the performance of convolutional and turbo-based BICM-ID systems. However, it is not required in LDPC and protograph-based counterparts because an inherent interleaver is involved in such types of codes [25], [26]. Particularly, LDPC and protograph-based BICM systems have lower implementation complexity than turbo-based counterparts because of the code construction and system architecture. Motivated by such an appealing feature, LDPC codes [27], [28] and protograph codes [29] have been intensely studied and optimized in BICM-ID systems over ergodic channels, such as additive white Gaussian noise (AWGN), fast-fading, and Poisson pulse-position modulation (PPM) channels. On the contrary, only the blockwise convolutional codes [30]–[32] and turbo-like codes [33] have been explored to match the BICM-NI systems in non-ergodic BF channels. More importantly, no related research works have provided effective solutions to devise outage-limit-approaching BICM-ID schemes in slow-fading scenarios. Apart from the ECCs, the performance of BICM systems is also dependent on the constellation labeling and bit-to-symbol (B2S) mapping because high-order modulations, e.g., M-ary phase shift keying (PSK) and quadrature amplitude modulation (QAM), are adopted. As such, these two techniques have been studied for both LDPC and protograph-based BICM-NI systems [34], [35] and BICM-ID systems [21], [27], [36] in order to further improve their overall performance. Nonetheless, all existing labeling and mapping rules are derived under ergodic AWGN and fast-fading channels, and therefore are no longer effective for non-ergodic BF channels.

To the best of our knowledge, there is a paucity of literature touching upon the feasibility of powerful LDPC codes in BICM systems, especially the BICM-ID systems, in BF environments. Although the convolutional and turbo-like-based BICM-NI systems have been studied in the context of BF channels [30]–[33], these two types of codes are inferior to the LDPC codes in either the performance or complexity aspect. Moreover, the above works have not mentioned the BICM-ID frameworks. In fact, how to design a bandwidth-efficient LDPC-based BICM system over BF channels is still a challenging problem today. As recalled, RP codes that enable simple structure and full diversity over BPSK-modulated BF channels can be viewed as a potential candidate for the BICM-ID systems. Against this background, we conduct a comprehensive investigation on the design of RP-based BICM-ID (referred to as *RP-BICM-ID*) systems with MPSK and MQAM constellations over non-ergodic BF channels. The proposed design method is a canonical framework which also works well with other types of modulations. The main contributions of this work are summarized as follows:

1) We propose a novel modulation strategy for the RP codes and formulate a bandwidth-efficient RP-BICM-ID system based on the non-ergodic property of BF channels. An attractive feature of the proposed RP-BICM-ID systems is that they can not only achieve full diversity but also boost the spectral efficiency

over BF channels.

2) We analyze the outage probability of RP-BICM-ID systems over BF channels. The outage probability establishes the fundamental lower-limit on the WER of RP-BICM-ID systems, and also provides an ultimate objective for their corresponding design under slow-fading environments.
3) We develop a multi-level PEXIT (ML-PEXIT) algorithm for the proposed RP-BICM-ID systems by exploiting the turbo-equalization principle so as to derive their asymptotic WER and BER over BF channels. We further find that the anti-Gray-labeled RP-BICM scheme can obtain remarkable performance gain by exploiting ID, while the Gray-labeled counterparts cannot do so.
4) We conceive an unequal-error-protection (UEP)-based B2S mapping scheme for the proposed RP-BICM-ID systems based on the rootcheck structure. The proposed UEP-B2S mapping scheme can accelerate the convergence speed of the RP decoder during the global iteration and thus make the proposed BICM-ID system achieve near-outage-limit performance.

The remainder of this paper is organized as follows. To begin with, we describe the system model and the proposed modulation strategy in Section II. Then, we analyze the outage-probability limit of the RP-BICM-ID systems over BF channels in Section III. In Section IV, we develop the ML-PEXIT algorithm and elaborate how to estimate the asymptotic WER and BER of RP-BICM-ID systems. In Section V, we introduce a novel UEP-B2S mapping scheme for the RP-BICM-ID systems. We give various numerical results in Section VI and concluding remarks in Section VII.

II. System Model and Modulation Strategy

In this section, we first introduce the principles of the RP-BICM-ID systems and the full-diversity RP-codes over BF channels. Following the above preliminary knowledge, we propose an efficient modulation strategy tailored for the RP-BICM-ID systems in such scenarios.

A. System Model

The RP-BICM-ID system to be studied in this paper is illustrated in Fig. 1. Consider a BF channel with L fading blocks, the information bits are encoded to an L-layer RP code [14], where the code rate and length equal $r_{\mathrm{RP}} = 1/L$ and N_{RP}, respectively. After that, every w coded bits are modulated into an MPSK or MQAM symbol ($w = \log_2 M$), and thus the overall codeword is converted to an M-ary modulated sequence of length $N'_{\mathrm{RP}} = N_{\mathrm{RP}}/w$.[2] The M-ary modulated sequence is then transmitted over a Nakagami-

[2]Note that although we assume the MPSK/MQAM as the modulation scheme in this paper, the proposed design is applicable to other modulation schemes, such as the amplitude-phase-shift keying (APSK) and pulse-amplitude modulation (PAM).

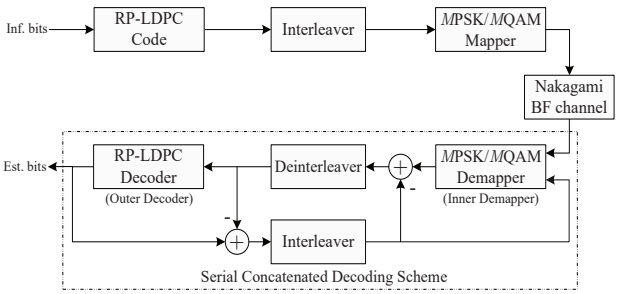

Fig. 1. Block diagram of an RP-BICM-ID system over a Nakagami BF channel.

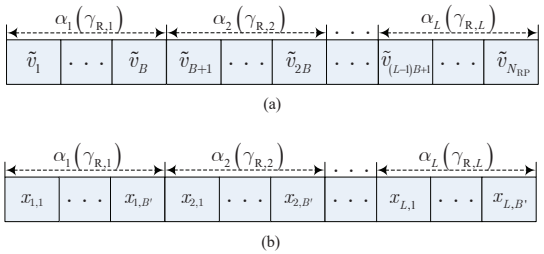

Fig. 2. Transmission mechanism of a rate-$1/L$ RP code in the BICM-ID system over a BF channel with L fading blocks: from the (a) bit-level perspective, i.e., $\Lambda_{\mathrm{RP}} = (\widetilde{v}_1, \widetilde{v}_2, \ldots, \widetilde{v}_{N_{\mathrm{RP}}})$ and (b) symbol-level perspective, i.e., $\mathbf{x}_{\mathrm{RP}} = (x_{1,1}, x_{1,2}, \ldots, x_{L,B'})$.

m BF channel with L fading blocks.[3] In this sense, each modulated sequence is affected by L independent fading gains. The number of symbols in each fading block, referred to as *block length*, equals $B' = N'_{\mathrm{RP}}/L$ (from the bit-level perspective, the block length equals $B = N_{\mathrm{RP}}/L$). For simplicity, we assume that N_{RP} is a common multiple of w and L. The transmission mechanism of an RP-BICM-ID system over a BF channel with L fading blocks is shown in Fig. 2.

With such a model, the received signal $y_{l,k}$ corresponding to the k-th transmitted symbol in the l-th block $x_{l,k} \in \chi$ can be expressed as

$$y_{l,k} = \alpha_l x_{l,k} + n_{l,k}, \tag{1}$$

where $l = 1, 2, \ldots, L$; $k = 1, 2, \ldots, B'$; χ is the constellation set and $|\chi| = M = 2^w$, $n_{l,k}$ is the complex Gaussian noise with zero mean and variance $\sigma_n^2 = N_0/2$ per dimension; $\alpha_l = |\alpha_l| \exp(j\varphi_l)$ is the complex channel fading gain; φ_l denotes the phase shift following a uniform distribution in $[-\pi, \pi]$ and $|\alpha_l|$ denotes the scalar fading gain following a Nakagami-m distribution. In particular, $|\alpha_l|$ is independent of φ_l. The probability density function (PDF) of $|\alpha_l|$ is given by

$$f_{|\alpha_l|}(\tau) = (2/\Gamma(m)) \, (m/\Omega)^m \, \tau^{2m-1} \exp\left(-(m\tau^2)/\Omega\right), \tag{2}$$

where Ω represents the expectation of τ^2 (i.e., the power of fading gain) and is assumed to be unity, i.e., $\Omega = \mathbb{E}[\tau^2] = 1$; $m \geq 1/2$ is the fading depth; and $\Gamma(\cdot)$ is the Gamma function.

[3]In this paper, we consider the Nakagami-m fading channel because it is a practical and generalized channel model that can suitably describe the fading statistics of various wireless communication environments. Moreover, Rayleigh fading channel ($m = 1$) and AWGN channel ($m \to \infty$) are two special cases of Nakagami-m fading channel [37].

At the receiver, the received signal is decoded by a serial concatenated framework, which is composed of a single-input single-output (SISO) demapper (inner demapper) and an SISO decoder (outer decoder). Unlike in the conventional BICM-NI systems, the extrinsic log-likelihood ratios (LLRs, also known as the soft information) of the demapper and decoder in the BICM-ID system are iteratively updated so as to accelerate the convergence and to improve the reliability of the a-posteriori LLRs. In such a framework, the extrinsic LLRs output from the decoder can be exploited by the demapper as the a-priori information, which is of great importance to boost the accuracy of decoded bits (i.e., estimated bits). In this work, we adopt a maximum a-posteriori (MAP) algorithm [17], [36] and a belief-propagation (BP) algorithm [12] to implement the demapper and the decoder, respectively. As is well known, any LDPC encoder (or protograph encoder) does include an inherent interleaver. Its error performance remains unchanged irrespective of the existence of interleaver [25], [38]. Consequently, we do not need to consider the interleaver module in the RP-BICM-ID systems. In this paper, we assume that the receiver can capture perfect channel state information (CSI) by exploiting an idea channel estimator unless otherwise specified.

The spectral efficiency of a BICM-ID system is defined as $R_{\mathrm{SE}} = r_{\mathrm{RP}} \log_2 M = r_{\mathrm{RP}} w$. In addition, the transmitted signal-to-noise-ratio (SNR) is defined as $\gamma_{\mathrm{T}} = E_{\mathrm{S}}/N_0$, while the received SNR of the l-th block is defined as $\gamma_{\mathrm{R},l} = |\alpha_l|^2 E_{\mathrm{S}}/N_0$, where E_{S} is the average energy per transmitted symbol and N_0 is the noise power spectral density. Unless otherwise stated, we will use "SNR" to represent "transmitted SNR". As there are totally L received SNRs in a BF channel, we can refer to $\boldsymbol{\gamma}_{\mathrm{R}} = (\gamma_{\mathrm{R},1}, \gamma_{\mathrm{R},2}, \ldots, \gamma_{\mathrm{R},L})$ as the received SNR profile. According to [37], one can easily show that the l-th received SNR follows a Gamma distribution, i.e., $\gamma_{\mathrm{R},l} \sim G(m, \gamma_{\mathrm{T}}/m)$. Therefore, the PDF of $\gamma_{\mathrm{R},l}$ is given by

$$f_{\gamma_{\mathrm{R},l}}(\tau) = [\tau^{m-1} \exp\left((-\tau)/(\gamma_{\mathrm{T}}/m)\right)]/[(\gamma_{\mathrm{T}}/m)^m \, \Gamma(m)], \quad \tau > 0. \tag{3}$$

As recalled, the diversity order achieved by a protograph code over a BF channel is defined as [1]

$$d = -\lim_{\gamma_{\mathrm{T}} \to \infty} (\ln P_{\mathrm{W}})/(\ln \gamma_{\mathrm{T}}), \tag{4}$$

where P_{W} is the word error rate (WER) of the protograph code at the decoder output. A protograph code can achieve full diversity over a Nakagami BF channel if the diversity order equals the product of the fading depth and the number of fading blocks, i.e., $d = mL$, where L is the maximum achievable diversity order provided by the code and m is the diversity order provided by the channel.

Furthermore, the achievable diversity order of a protograph code in BICM-ID systems over a Nakagami BF channel is limited by the Singleton bound [30], [33], i.e.,

$$d \leq m \left(1 + \lfloor L \left(1 - (R_{\mathrm{SE}}/\log_2 |\chi|)\right) \rfloor\right), \tag{5}$$

where $|\chi|$ is the cardinality of χ. The protograph code is referred to as a maximum-distance separable (MDS) code if it can perfectly achieve the Singleton-like bound. Because $d \leq m \left(1 + \lfloor L \left(1 - (R_{\mathrm{SE}}/\log_2 |\chi|)\right) \rfloor\right) \leq$

mL, a full-diversity protograph code is an MDS code (where the code rate $r_{\rm RP} \leq 1/L$), but an MDS code may not be a full-diversity code. For simplicity, we will refer to a full-diversity MDS protograph code as a full-diversity protograph code in the remainder of this paper. The Singleton bound suggests the optimal tradeoff between the code rate and diversity order. As indicated in (5), $r_{\rm RP,max} = 1/L$ (resp. $R_{\rm SE,max} = \log_2|\chi|/L = w/L$) is the highest achievable code rate (resp. spectral efficiency) for a full-diversity protograph code in BICM-ID systems (resp. protograph-based BICM-ID system).

Remark: In accordance with the Singleton-like bound, it is possible to design MDS protograph codes with rates higher than $1/L$, which benefit from spectral efficiencies higher than w/L (i.e., $R_{\rm SE} = \log_2|\chi|/r_{\rm RP} > w/L$) in BICM-ID systems. However, such MDS codes can no longer achieve full diversity and thus suffers from non-trivial performance loss as compared with the full-diversity protograph codes, especially in the high-SNR region. Due to the above reason, MDS protograph codes with rates higher than $1/L$ may not be able to satisfy the ultra-high-reliability requirement in future wireless communication applications.

B. Full-Diversity RP codes

As a special case of Tanner graph, a protograph consists of relatively few nodes and edges [12]. Specifically, a protograph can be denoted by $\mathcal{G} = (\mathcal{V}, \mathcal{C}, \mathcal{E})$, where $\mathcal{V}$ is the variable-node (VN) set with $n_{\rm RP}$ elements, $\mathcal{C}$ is the check-node (CN) set with $m_{\rm RP}$ elements, and $\mathcal{E}$ is the edge set connecting the VNs to the CNs. For example, an edge $e_{i,j} \in \mathcal{E}$ connects the j-th VN $\widetilde{v}_j \in \mathcal{V}$ to the i-th CN $\widetilde{c}_i \in \mathcal{C}$. The main difference between the protograph and Tanner graph is that parallel edges can be involved in the former. Also, a protograph can be specified by an $m_{\rm RP} \times n_{\rm RP}$ base matrix $\mathbf{H}_{\rm B} = (h_{i,j})$, in which $h_{i,j}$ represents the number of edges connecting $\widetilde{v}_j$ to $\widetilde{c}_i$. Based on the size of protograph or base matrix, the code rate is obtained, i.e., $R_{\rm RP} = (n_{\rm RP} - m_{\rm RP})/n_{\rm RP}$. An $M_{\rm RP} \times N_{\rm RP}$ expanded protograph (referred to as *derived graph*), which corresponds to the parity matrix of a protograph code of length $N_{\rm RP}$, can be constructed by "lifting" the protograph, where $Z \triangleq N_{\rm RP}/n_{\rm RP} = M_{\rm RP}/m_{\rm RP}$ is the lifting factor. In general, the lifting procedure can be implemented via a modified PEG algorithm [39].

The RP codes, which were introduced in [12], are a type of structured protograph codes that can not only achieve full diversity over BF channels but also possess maximum code rate. As the fundamental basis of RP code, *root CNs (called rootchecks)* guarantee that all information bits achieve full-diversity performance over BF channels. Consider an L-layer RP code transmitted over a BF channels with L fading blocks. A degree-ρ_i ($\rho_i \geq 3$) type-l rootcheck is defined as a CN having single edge connecting to an information-bit-related VN $v_{\rm il}$ transmitted on the l-th fading gain, and the remaining $\rho_i - 1$ edges connecting to the VNs transmitted on one of the other $L-1$ fading gains.

Remark: To ensure full diversity of $v_{\mathrm{i}l}$, this VN must connect to $m_{\mathrm{RC}} = L-1$ different type-l rootchecks, which are referred to as *type-l rootcheck set*. In particular, the l'-th ($l' = 1, \ldots, l-1, l+1, \ldots, L$) type-$l$ rootcheck is defined as the CN having single edge connecting to $v_{\mathrm{i}l}$ and the remaining $\rho_i - 1$ edges connecting to the VNs transmitted on $\alpha_{l'}$.

An L-layer full-diversity RP code $\Lambda_{\mathrm{RP}} = (\mathcal{V}_1, \mathcal{V}_2, \ldots, \mathcal{V}_L)$ is constructed based on its L types of rootcheck sets, where $\mathcal{V}_l$ is the l-th coded-bit set (i.e., VN set) of the code. Assume that the protograph of $\mathcal{V}_{\mathrm{RP}}$ includes n_{RP} VNs and m_{RP} CNs. For the protograph, there are totally $B = n_{\mathrm{RP}}/L$ VNs in each VN set. In the BF channel, the l-th VN set $\mathcal{V}_l$ is transmitted on the l-th fading gain α_l. To enable strong robustness against block fading, the RP code design must be symmetric for all L VN sets and L rootcheck sets. In other words, the RP code must still achieve full diversity if the order of fading gains randomly permutes. To this end, there must be L different types of rootcheck sets in an L-layer RP code. Based on the aforementioned analysis, the $m_{\mathrm{RP}} \times n_{\mathrm{RP}}$ general base matrix of Λ_{RP} can be expressed by

$$\mathbf{H}_{\mathrm{B,RP}} = \begin{array}{c} \begin{array}{cccccccccc} \mathcal{V}_{\mathrm{i}1} & \mathcal{V}_{\mathrm{p}1} & & \mathcal{V}_{\mathrm{i}2} & \mathcal{V}_{\mathrm{p}2} & & \cdots & \cdots & \mathcal{V}_{\mathrm{i}L} & \mathcal{V}_{\mathrm{p}L} \end{array} \\ \left(\begin{array}{cc|cc|c|cc|cc} \mathbf{1} & \mathbf{0} & \mathbf{H}_{\mathrm{i}2,1} & \mathbf{H}_{\mathrm{p}2,1} & \cdots & \cdots & \mathbf{H}_{\mathrm{i}L,1} & \mathbf{H}_{\mathrm{p}L,1} \\ \mathbf{H}_{\mathrm{i}1,1} & \mathbf{H}_{\mathrm{p}1,1} & \mathbf{1} & \mathbf{0} & \cdots & \cdots & \cdots & \cdots \\ \cdots & \cdots & \cdots & \cdots & \cdots & \cdots & \mathbf{H}_{\mathrm{i}L,L-1} & \mathbf{H}_{\mathrm{p}L,L-1} \\ \mathbf{H}_{\mathrm{i}1,L-1} & \mathbf{H}_{\mathrm{p}1,L-1} & \mathbf{H}_{\mathrm{i}2,L-1} & \mathbf{H}_{\mathrm{p}2,L-1} & \cdots & \cdots & \mathbf{1} & \mathbf{0} \end{array}\right) \begin{array}{c} \mathcal{C}_1 \\ \mathcal{C}_2 \\ \cdots \\ \mathcal{C}_L \end{array} \end{array} \tag{6}$$

where $\mathbf{1}$ represents the all-one vector of size $(L-1) \times 1$; $\mathbf{0}$ represents the all-zero matrix of size $(L-1) \times (L-1)$; $\mathbf{H}_{\mathrm{i}l,\mu}$ $(l = 1, 2, \ldots, L; \mu = 1, 2, \ldots, L-1)$ represents a sub-matrix of size $(L-1) \times 1$; $\mathbf{H}_{\mathrm{p}l,\mu}$ represents a sub-matrix of size $(L-1) \times (L-1)$; the VN set $\mathcal{V}_l = (\mathcal{V}_{\mathrm{i}l}, \mathcal{V}_{\mathrm{p}l}) = (v_{\mathrm{i}l}, v_{\mathrm{p}l,1}, \ldots, v_{\mathrm{p}l,L-1})$ in the l-th fading block is divided into two subsets, with $\mathcal{V}_{\mathrm{i}l}$ and $\mathcal{V}_{\mathrm{p}l}$ being the information-bit-related VNs and parity-bit-related VNs, respectively; $\mathcal{C}_l = (c_{l,1}, \ldots, c_{l,l-1}, c_{l,l+1}, \ldots, c_{l,L})$ denotes the type-l rootcheck set, which corresponds to the sub-base-matrix $\mathbf{H}_{\mathcal{C}_l} = (\mathbf{H}_{\mathrm{i}1,l-1}\, \mathbf{H}_{\mathrm{p}1,l-1} \cdots \mathbf{H}_{\mathrm{i}(l-1),l-1}\, \mathbf{H}_{\mathrm{p}(l-1),l-1}\, \mathbf{1}\ \mathbf{0}\ \mathbf{H}_{\mathrm{i}(l+1),l}$ $\mathbf{H}_{\mathrm{p}(l+1),l} \cdots \mathbf{H}_{\mathrm{i}L,l}\, \mathbf{H}_{\mathrm{p}L,l})$; $n_{\mathrm{RP}} = L^2$ is the number of VNs (i.e., codeword length); $m_{\mathrm{RP}} = (L-1)L$ is the number of CNs; $k_{\mathrm{RP}} = n_{\mathrm{RP}} - m_{\mathrm{RP}} = L$ is the information length. Hence, the code rate equals $r_{\mathrm{RP}} = 1/L$.

In the protograph of the RP code, the overall VN set and CN set are expressed by $\mathcal{V}_{\mathrm{RP}}{=}(\mathcal{V}_1, \mathcal{V}_2, \ldots, \mathcal{V}_L)$ and $\mathcal{C}_{\mathrm{RP}} = (\mathcal{C}_1, \mathcal{C}_2, \ldots, \mathcal{C}_L)$, respectively. Based on the design method, the information bits are clearly distinguished from the parity bits in an RP code. It has been proved in [14] that the information bits in an RP code can accomplish the full-diversity order under BP decoding at the price of degrading the diversity order of the parity bits. In other words, the information bits are protected with a relatively higher priority compared with the parity bits, which is referred to as *UEP property*. This property is very promising in practice because the error performance is only measured by the accuracy of information bits.

To clearly illustrate the potential benefit of the proposed RP-BICM-ID framework, we will restrict our attention to the hardware-friendly regular RP codes, in which both the VN degree and CN degree are constants. Nonetheless, it is easy to construct irregular RP codes based on the above construction method, readers who are interested can refer to [14] for more details.

Example 1 – Base Matrices of RP codes. The base matrices of a rate-$1/2$ regular-$(3, 6)$ bilayer RP code, a rate-$1/3$ regular-$(4, 6)$ three-layer RP code, and a rate-$1/4$ regular-$(6, 8)$ four-layer RP code are shown as

$$\mathbf{H}_{\text{B,RP-2}} = \begin{pmatrix} 1\,0 & 2\,3 \\ 2\,3 & 1\,0 \end{pmatrix}, \quad \mathbf{H}_{\text{B,RP-3}} = \begin{pmatrix} 1\,0\,0 & 1\,2\,2 & 0\,0\,0 \\ 1\,0\,0 & 0\,0\,0 & 1\,2\,2 \\ 1\,2\,2 & 1\,0\,0 & 0\,0\,0 \\ 0\,0\,0 & 1\,0\,0 & 1\,2\,2 \\ 1\,2\,2 & 0\,0\,0 & 1\,0\,0 \\ 0\,0\,0 & 1\,2\,2 & 1\,0\,0 \end{pmatrix}, \quad \mathbf{H}_{\text{B,RP-4}} = \begin{pmatrix} 1\,0\,0\,0 & 1\,2\,2\,2 & 0\,0\,0\,0 & 0\,0\,0\,0 \\ 1\,0\,0\,0 & 0\,0\,0\,0 & 1\,2\,2\,2 & 0\,0\,0\,0 \\ 1\,0\,0\,0 & 0\,0\,0\,0 & 0\,0\,0\,0 & 1\,2\,2\,2 \\ 1\,2\,2\,2 & 1\,0\,0\,0 & 0\,0\,0\,0 & 0\,0\,0\,0 \\ 0\,0\,0\,0 & 1\,0\,0\,0 & 1\,2\,2\,2 & 0\,0\,0\,0 \\ 0\,0\,0\,0 & 1\,0\,0\,0 & 0\,0\,0\,0 & 1\,2\,2\,2 \\ 1\,2\,2\,2 & 0\,0\,0\,0 & 1\,0\,0\,0 & 0\,0\,0\,0 \\ 0\,0\,0\,0 & 1\,2\,2\,2 & 1\,0\,0\,0 & 0\,0\,0\,0 \\ 0\,0\,0\,0 & 0\,0\,0\,0 & 1\,0\,0\,0 & 1\,2\,2\,2 \\ 1\,2\,2\,2 & 0\,0\,0\,0 & 0\,0\,0\,0 & 1\,0\,0\,0 \\ 0\,0\,0\,0 & 1\,2\,2\,2 & 0\,0\,0\,0 & 1\,0\,0\,0 \\ 0\,0\,0\,0 & 0\,0\,0\,0 & 1\,2\,2\,2 & 1\,0\,0\,0 \end{pmatrix}. \quad (7)$$

The above three types of RP codes are referred to as *RP-*2 *code, RP-*3 *code,* and *RP-*4 *code*, respectively, where the digit appended to "RP" is used to denote the number of layers of an RP code. In accordance with the construction principle of RP codes, the RP-2 code, RP-3 code, and RP-4 code can achieve the full-diversity performance over BF channels with two fading blocks, three fading blocks, and four fading blocks, respectively.

C. Modulation Strategy for RP-BICM-ID Systems

As described in Sect. II-B, an L-layer root protograph includes L^2 VNs and $L(L-1)$ CNs. One can generate an RP code of length ZL^2 $(B = ZL)$ by lifting the $(L(L-1)) \times L^2$ root protograph to a $(ZL(L-1)) \times (ZL^2)$ derived graph, where Z is the lifting factor. To facilitate the design and analysis, we define an intermediate protograph as a $(qL(L-1)) \times (qL^2)$ protograph lifted by the original protograph, where q is a relatively small positive integer (i.e., $1 < q \ll Z$).

Given an intermediate protograph, there are q copies of the VN set $\mathcal{V}_l$, denoted by $\mathcal{V}_{\text{IP},l} = (\mathcal{V}_{l,1}, \mathcal{V}_{l,2}, \ldots, \mathcal{V}_{l,q})$, in the l-th fading block, where $\mathcal{V}_{l,\mu} = \mathcal{V}_{\text{i}l,\mu} \cup \mathcal{V}_{\text{p}l,\mu}$ $(\mu = 1, 2, \ldots, q)$. In particular, $\mathcal{V}_{\text{i}l,\mu}$ and $\mathcal{V}_{\text{p}l,\mu}$ include the single information bit and $(L-1)$ parity bits, respectively. Unlike ergodic channels, the modulation order, i.e., $M = 2^w$ $(w = 2, 3, \ldots)$, over non-ergodic BF channels must be carefully selected so as to retain the

full-diversity property of RP codes in BICM-ID systems. Note that BPSK has been discussed in our previous work [14] and is not discussed here. Without loss of generality, given fixed q and L, we elaborate three possible cases for the selection of modulation order (i.e., modulation strategy) based on the relationship between w and qL as follows.

Case 1 ($\boldsymbol{w = qL}$): The l-th VN set $\mathcal{V}_{\mathrm{IP},l}$ of the intermediate protograph can be mapped onto an M-ary symbol $x_l = \{b_{l_1}, b_{l_2}, \ldots, b_{l_w}\}$ transmitted on the same fading gain (i.e., α_l). The overall l-th VN set $\mathcal{V}_l = \{\mathcal{V}_{l,1}, \mathcal{V}_{l,2}, \ldots, \mathcal{V}_{l,Z}\} = \{\mathcal{V}_{\mathrm{IP},1}, \mathcal{V}_{\mathrm{IP},2}, \ldots, \mathcal{V}_{\mathrm{IP},Z'}\}$ in the RP code is mapped onto an M-ary sequence $\mathbf{x}_l = \{x_{l,1}, x_{l,2}, \ldots, x_{l,Z'}\}$ transmitted on α_l, where $Z' = Z/q$ and $\mathbf{x}_l$ is referred to as *the l-th symbol set* of the overall RP code. In this case, the system can not only realize high spectral efficiency (i.e., $R_{\mathrm{SE}} = r_{\mathrm{RP}} w = q$) but also achieve full-diversity performance.

Case 2 ($\boldsymbol{w > qL}$): If $w - qL$ extra "0" bits are inserted into the l-th VN set of the intermediate protograph, the modified l-th VN set comprising w VNs can be mapped onto an M-ary symbol transmitted on the same fading gain (i.e, α_l). In this situation, the full-diversity property and spectral efficiency (i.e., $R_{\mathrm{SE}} = q$) can be retained by exploiting a higher modulation order and longer block length, which leads to higher complexity and higher latency; otherwise, if no extra "0" bits are inserted into the l-th VN set, $w - qL$ VNs transmitted on α_{l+1} should be appended to the l-th VN set so as to formulate the w bits being mapped to the M-ary symbol transmitted on α_l. In this situation, the full-diversity property (i.e., the rootcheck structure) will vanish because the VNs mapped onto an M-ary symbol span two different VN sets.

Case 3 ($\boldsymbol{w < qL}$): If $(qL) \mod w = 0$, the l-th VN set of the intermediate protograph can be mapped onto qL/w M-ary symbols transmitted on α_l; otherwise, i.e., $(qL) \mod w \neq 0$, the qL bits included in the l-th VN set together with $\lceil (qL)/w \rceil w - qL$ extra "0" bits must be mapped onto $\lceil (qL)/w \rceil$ M-ary symbols transmitted on α_l. Although the full-diversity of RP code can be preserved in both situations, the spectral efficiency is not satisfactory (i.e., $R_{\mathrm{SE}} = q/\lceil (qL)/w \rceil$). Especially, the spectral efficiency of the latter situation is worse than that of the former situation because some redundancy is included.

Based on the above discussion, the three possible cases for the modulation strategy are illustrated in Fig. 3. Therefore, with an aim to achieving not only high transmission reliability but also high spectral efficiency and low complexity, the modulation order must be a power function of 2^L, i.e., $M = 2^w = (2^L)^q = 2^{qL}$ (i.e., **Case 1** must be selected). In general, for an L-layer RP code transmitted over a BF channel with L fading blocks, we adopt 2^{qL}-PSK/QAM as the modulation scheme. Exploiting the proposed modulation scheme, the spectral efficiency of the RP-BICM-ID system is $R_{\mathrm{SE}} = (qL) \times r_{\mathrm{RP}} = (qL)/L = q$. In the RP-BICM-ID systems, we adopt MPSK if $M \leq 8$ and adopt MQAM otherwise. For instance, Fig. 4 shows the constellations of QPSK, 8PSK and 16QAM with both Gray labeling and anti-Gray labeling.

Although we only consider these two labelings in this paper, our analysis and design approaches are also

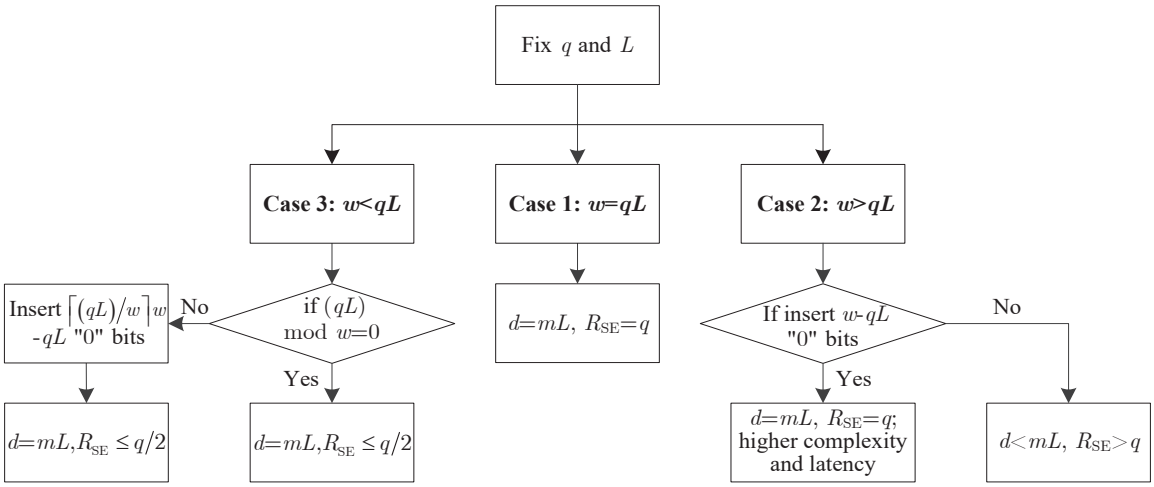

Fig. 3. Graphical description of the three possible cases for the modulation strategy of RP-BICM-ID systems. Please move Case 3 to the right-most.

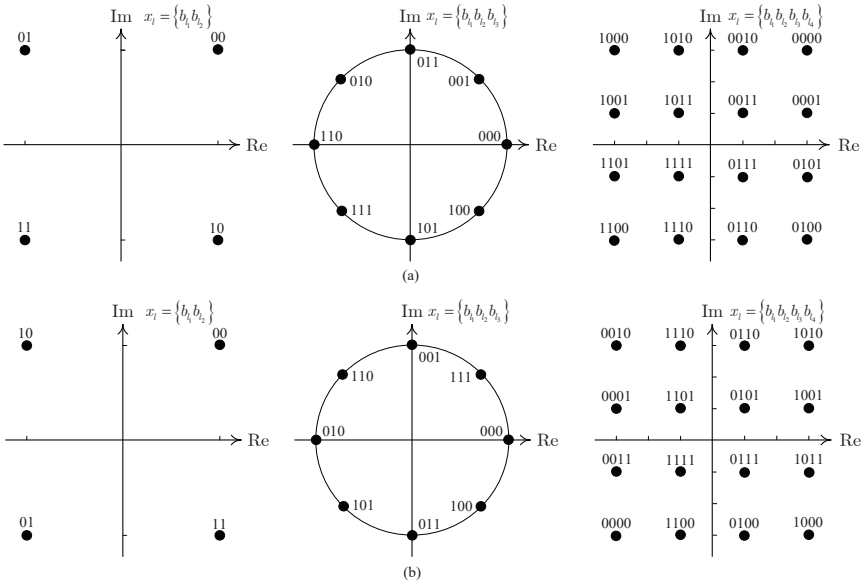

Fig. 4. Constellations of the QPSK, 8PSK and 16QAM: (a) Gray labeling and (b) anti-Gray labeling.

applicable to other labeling rules, such as set-partitioning labeling [18]. Unless otherwise stated, we will assume $q = 1$ (i.e., $w = L$) for the analysis and optimization of RP-BICM-ID systems to ease the exposition. The proposed method can be easily generalized to $q > 1$.

III. Outage-Probability-Limit Analysis

Different from ergodic AWGN and fast-fading channels, the non-ergodic BF channel is not information stable and thus its Shannon capacity equals zero. For this reason, Shannon capacity cannot be utilized to specify the performance limit of a BF channel. To resolve the above problem, the information outage probability has been introduced to characterize the information-theoretical lower limit on the WER of any ECC with sufficiently large codeword length [1]. To the best of our knowledge, no research effort has been devoted to analyzing the outage probability of BICM-ID systems with the complex-valued MPSK/MQAM

signaling over a BF channel. In this section, we put forward the derivation of such performance limit from the information-theoretical perspective.

For a given BF channel, an outage event occurs if the instantaneous mutual information $I_{\mathrm{BF}}(\gamma_{\mathrm{T}}, \boldsymbol{\alpha})$ is smaller than the spectral efficiency R_{SE}, i.e., $I_{\mathrm{BF}}(\gamma_{\mathrm{T}}, \boldsymbol{\alpha}) < R_{\mathrm{SE}}$. In particular, the instantaneous mutual information is dependent on the channel realization, i.e., both the transmitted SNR γ_{T} and the fading profile $\boldsymbol{\alpha} = (\alpha_1, \alpha_2, \ldots, \alpha_l)$. As the fading gains of the L blocks are independent of one another, the transmission of an RP codeword over a BF channel with L fading blocks can be viewed as the transmissions of L VN (i.e., coded-bit) sets through L parallel AWGN channels. In this sense, the mutual information of such a BF channel equals the average mutual information of L independent AWGN channels, and can be written as

$$I_{\mathrm{BF}}(\gamma_{\mathrm{T}}, \boldsymbol{\alpha}) = \frac{1}{L}\sum_{l=1}^{L} I_{\mathrm{AWGN}}(\gamma_{\mathrm{T}}|\alpha_l|^2) = \frac{1}{L}\sum_{l=1}^{L} I_{\mathrm{AWGN}}(\gamma_{\mathrm{R},l}), \tag{8}$$

where $I_{\mathrm{AWGN}}(\tau)$ represents the input-output mutual information of an equivalent AWGN channel with a transmitted SNR per symbol equal to τ. Precisely speaking, the instantaneous mutual information of the l-th fading block can be viewed as the mutual information of the l-th equivalent AWGN channel with an SNR equal to $\gamma_{\mathrm{R},l}$. For the l-th equivalent AWGN channel, we define the SNR by $\gamma_{\mathrm{T},l}^{(\mathrm{Eq})} \triangleq E_{\mathrm{S},l}^{(\mathrm{Eq})}/N_{0,l}^{(\mathrm{Eq})} = \gamma_{\mathrm{R},l}$, where $E_{\mathrm{S},l}^{(\mathrm{Eq})}$ and $N_{0,l}^{(\mathrm{Eq})}$ are the average energy per transmitted symbol and the noise power spectral density. Suppose that $E_{\mathrm{S},l}^{(\mathrm{Eq})}$ is normalized to unity, the variance of Gaussian noise per dimension can be formulated as

$$\left(\sigma_{n,l}^{(\mathrm{Eq})}\right)^2 = N_{0,l}^{(\mathrm{Eq})}/2 = 1/(2\gamma_{\mathrm{T},l}^{(\mathrm{Eq})}) = 1/(2\gamma_{\mathrm{R},l}). \tag{9}$$

Thus, the outage probability is defined as

$$P_{\mathrm{out}}\left(\gamma_{\mathrm{T}}, \boldsymbol{\alpha}\right) = \Pr\left(I_{\mathrm{BF}}(\gamma_{\mathrm{T}}, \boldsymbol{\alpha}) < R_{\mathrm{SE}}\right) = \Pr\left(\sum_{l=1}^{L} I_{\mathrm{AWGN}}(\gamma_{\mathrm{R},l}) < LR_{\mathrm{SE}}\right). \tag{10}$$

One the one hand, assume that an M-ary coded-modulation (CM) signal is transmitted over an AWGN channel with an SNR $\gamma_{\mathrm{T},l}^{(\mathrm{Eq})} = \gamma_{\mathrm{R},l}$, the input-output mutual information can be measured as

$$I_{\mathrm{AWGN-CM}}(\gamma_{\mathrm{R},l}) = w - \mathbb{E}_{x,y}\left[\log_2 \frac{\sum_{x'\in\chi} f(y_l|x_l = x')}{f(y_l|x_l)}\right], \tag{11}$$

where $x \in \chi$ and $|\chi| = M$. With this model, the PDF $f(y_l|x_l)$ is expressed as

$$f(y_l|x_l) = \frac{1}{2\pi\left(\sigma_{n,l}^{(\mathrm{Eq})}\right)^2}\exp\left(-\frac{|y_l - x_l|^2}{2\left(\sigma_{n,l}^{(\mathrm{Eq})}\right)^2}\right). \tag{12}$$

As mentioned in [38], CM can realize error-free transmission with the maximum achievable rate, and thus it is an optimal transmission scheme.

On the other hand, for a BICM-NI system, the corresponding mutual information becomes [15]

$$I_{\mathrm{AWGN-BICM-NI}}(\gamma_{\mathrm{R,l}}) = w - \sum_{\mu=1}^{w}\mathbb{E}_{\varepsilon,y}\left[\log_2 \frac{\sum_{x'\in\chi} f(y_l|x_l = x')}{\sum_{x'\in\chi_\mu^\varepsilon} f(y_l|x_l = x')}\right] \tag{13}$$

where χ_μ^ε is the constellation signal with the μ-th component bit being $\varepsilon \in \{0, 1\}$. Since the w bits within each symbol are demapped independently, BICM cannot maximize the achievable rate and thus

belongs to a suboptimal transmission scheme. As a result, one can easily prove that $I_{\mathrm{AWGN-BICM-NI}}(\gamma_{\mathrm{R},l}) \leq I_{\mathrm{AWGN-CM}}((\gamma_{\mathrm{R},l})$.

In a BICM-ID system, i.e., an enhanced version of BICM-NI system, each bit is estimated by exploiting the a-priori information of the remaining $w-1$ bits within the same symbol (such information is fed back from the outer decoder). Consequently, BICM-ID can effectively compensate the rate loss of BICM-NI and achieve the maximum achievable rate [16], [17]. As such, the BICM-ID can be viewed as an optimal transmission scheme and hence $I_{\mathrm{AWGN-BICM-ID}}(\gamma_{\mathrm{R},l}) = I_{\mathrm{AWGN-CM}}(\gamma_{\mathrm{R},l})$.

Remark: Although it is impossible to derive closed-form expression of (11) and (13), one can resort to the Monte-Carlo method so as to numerically calculate the mutual information.

Based on the above discussions, we can first exploit (11) to calculate the mutual information of the BICM-ID system in the L different fading blocks. Subsequently, the outage region corresponding to the outage event $I_{\mathrm{BF-BICM-ID}}(\gamma_{\mathrm{T}}, \boldsymbol{\alpha}) < R_{\mathrm{SE}}$, i.e., $\sum_{l=1}^{L} I_{\mathrm{AWGN-BICM-ID}}(\gamma_{\mathrm{R},l}) < LR_{\mathrm{SE}}$, can be computed as

$$\overline{D}_{\mathrm{out-BICM-ID}} = \left\{ \boldsymbol{\gamma}_{\mathrm{R}} \in \mathcal{R}_{+}^{L} \mid \sum_{l=1}^{L} I_{\mathrm{AWGN-BICM-ID}}(\gamma_{\mathrm{R},l}) < LR_{\mathrm{SE}} \right\}, \tag{14}$$

where the surface $\gamma_{\mathrm{R},L} = \Xi(\gamma_{\mathrm{R},1}, \gamma_{\mathrm{R},2}, \ldots, \gamma_{\mathrm{R},L-1})$ satisfying $\sum_{l=1}^{L} I_{\mathrm{AWGN-BICM-ID}}(\gamma_{\mathrm{R},l}) = LR_{\mathrm{SE}}$ is defined as the outage boundary.

Finally, the outage probability of the BICM-ID system over a BF channel can be estimated by using

$$\begin{aligned} P_{\mathrm{out-BICM-ID}}(\boldsymbol{\gamma}_{\mathrm{R}}, R_{\mathrm{SE}}) &= Pr(I_{\mathrm{BF-BICM-ID}}(\boldsymbol{\gamma}_{\mathrm{R}}) < LR_{\mathrm{SE}}) \\ &= \int\int\cdots\int_{\bar{D}_{\mathrm{out-BICM-ID}}} f(\gamma_{\mathrm{R},1}) f(\gamma_{\mathrm{R},2}) \cdots f(\gamma_{\mathrm{R},L}) d\gamma_{\mathrm{R},1} d\gamma_{\mathrm{R},2} \cdots d\gamma_{\mathrm{R},L}. \end{aligned} \tag{15}$$

Note also that the outage probability of the BICM-NI system can be measured through a similar way (i.e., by substituting the outage region of BICM-NI system into (15)).

Example 2 – Outage Limits of BICM Systems. Using a rate-$1/2$ RP code and two modulation schemes (i.e., QPSK and 16QAM), we calculate the outage limits and outage boundaries of the BICM-ID and BICM-NI systems over a Nakagami BF channel with two fading blocks and show the corresponding results in Fig. 5. According to the expressions of mutual information in (11) and (13), the outage limit of the BICM-ID system is independent of the labeling while that of the BICM-NI system is dependent on the labeling. As seen from Fig. 5, the outage limits of the Gray-labeled BICM-NI system are very close to those of its corresponding BICM-ID system, while the outage limits of anti-Gray-labeled BICM-NI system are farther from those of its corresponding BICM-ID system. Especially, the outage limits of the Gray-labeled BICM-NI system and BICM-ID system overlap with each other for the QPSK modulation. In actual implementation, Gray labeling can maximize the soft information in each fading block (i.e., each equivalent AWGN channel) without an iterative receiver and hence it achieves very desirable error performance in such a scenario. Yet, it may obtain trivial gain by means of ID [40]. Although the anti-Gray-labeled BICM system is inferior to the

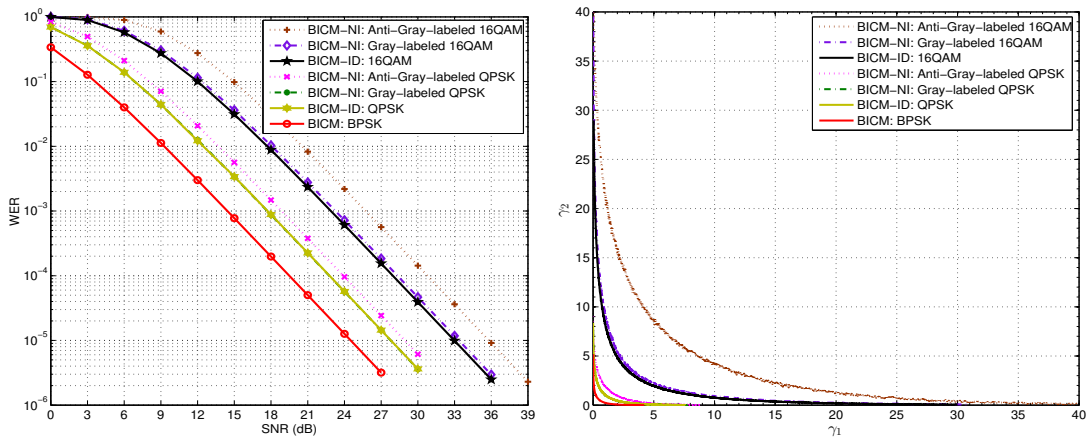

(a) (b)

Fig. 5. The (a) outage limits and (b) outage boundaries of the BICM-NI and BICM-ID systems over a Nakagami BF channel. The parameters used are $r_{\rm RP} = 1/2, M = 4, 16, m = 1,$ and $L = 2$.

TABLE I

VARIATIONS OF MATHEMATICAL NOTATIONS FOR VNS, CNS, AND TRANSMITTED SYMBOLS USED IN THIS PAPER.

Notation	Indication
$\mathcal{V}$	The overall VN set of an RP code
$\mathcal{V}_l$	The l-th VN set (i.e., the VN set affected by α_l)
$\mathcal{V}_{{\rm i}l}$	The l-th information-bit-related VN set
$\mathcal{V}_{{\rm p}l}$	The l-th parity-bit-related VN set
$\widetilde{v}_j$	The j-th VN in $\mathcal{V}$
$v_{l,\mu}$	The μ-th VN in $\mathcal{V}_l$
$\mathcal{C}$	The overall CN set of an RP code
$\mathcal{C}_l$	The l-th CN set (i.e., the CN set affected by α_l)
$\widetilde{c}_i$	The i-th CN in $\mathcal{C}$
$c_{l,\mu'}$	The μ'-th VN in $\mathcal{C}_l$
$\mathbf{x}_{\rm RP}$	The transmitted symbol sequence mapped from $\mathcal{V}$
x_l	The l-th transmitted symbol mapped from $\mathcal{V}_l$
$\widetilde{b}_j$	The j-th bit within $\mathbf{x}_{\rm RP}$
$b_{l,\mu}$	The μ-th bit within x_l

Gray-labeled BICM system without ID under BF condition, the former may acquire significant performance gain by means of ID and outperform the latter. We will further investigate the performance of RP-BICM-ID systems with different labelings over BF channels to verify the above conjecture in Sect. VI.

IV. ASYMPTOTIC PERFORMANCE ANALYSIS OF RP-BICM-ID SYSTEMS

A. Theoretical Foundation of LLR and Mutual-Information Calculations

We consider a BICM-ID system over a BF channel with L fading blocks, in which the code used is an L-layer RP code and the modulation adopted is an MPSK/MQAM with $M = 2^w = 2^L$. The

corresponding protograph consists of $n_{\rm RP}$ VNs and $m_{\rm RP}$ CNs, where the $n_{\rm RP} = BL = L^2$ and $m_{\rm RP} = L(L-1)$. Let $\mathcal{V}_l = (v_{\rm il}, v_{{\rm p}l,1}, , v_{{\rm p}l,2}, \ldots, v_{{\rm p}l,L-1}) \triangleq (v_{l,1}, v_{l,2}, v_{l,3}, \ldots, v_{l,L})$ be the l-th VN set and $\mathcal{C}_l = (c_{l,1}, \ldots, c_{l,l-1}, c_{l,l+1}, \ldots, c_{l,L})$ be the type-l rootcheck set. Assume that the L VNs in the l-th VN set are mapped onto an M-ary symbol $x_l = (b_{l_1}, b_{l_2}, \ldots, b_{l_w})$ in a sequential order prior to being transmitted on α_l, where $b_{l_\mu} = v_{l,\mu}$ is the μ-th component bit within the symbol. As a result, we can re-define the overall VN set and CN set of an RP code as follows: 1) the overall VN set in a code is $\mathcal{V}_{\rm RP} = (\mathcal{V}_1, \mathcal{V}_2, \ldots, \mathcal{V}_L) = (v_{1,1}, v_{1,2}, \ldots, v_{1,L}; \ldots; v_{L,1}, v_{L,2}, \ldots, v_{L,L}) = (\widetilde{v}_1, \widetilde{v}_2, \ldots, \widetilde{v}_{n_{\rm RP}})$, where $\widetilde{v}_j \triangleq v_{l,\mu}$ and $j = (l-1)L + \mu$ $(l = 1, 2, \ldots, L; \mu = 1, 2, \ldots, L)$; 2) $\mathcal{C}_{\rm RP} = (\mathcal{C}_1, \mathcal{C}_2, \ldots, \mathcal{C}_L) = (c_{1,2}, c_{1,3}, \ldots, c_{1,L}; \ldots; c_{L,1}, c_{L,2}, \ldots, c_{L,L-1}) = (\widetilde{c}_1, \widetilde{c}_2, \ldots, \widetilde{c}_{m_{\rm RP}})$, where $\widetilde{c}_i \triangleq c_{l,\mu'}, i = (l-1)(L-1) + \mu'$ if $\mu' < l,$ and $i = (l-1)(L-1) + \mu' - 1$ if $\mu' > l$, $\mu' = 1, 2, \ldots, L$. Besides, the transmitted symbol sequence corresponding to an RP code can be re-written as $\mathbf{x}_{\rm RP} = (x_1, x_2, \ldots, x_L) = (b_{1_1}, b_{1_2}, \ldots, b_{1_w}; \ldots, b_{L_1}, b_{L_2}, \ldots, b_{L_w}) = (\widetilde{b}_1, \widetilde{b}_2, \ldots, \widetilde{b}_{n_{\rm RP}})$, where the relationship between b_{l_μ} and $\widetilde{b}_j$ is identical to that between $v_{l,\mu}$ and $\widetilde{v}_j$. In summary, the variations of mathematical notations for VNs, CNs, and transmitted symbols used in this paper are listed in Table I. Note that the notations whose subscripts include the parameter "l" are defined in the context of BF channels, while the remaining notations are defined without considering the effect of BF channels.

To facilitate the description of ML-PEXIT algorithm and WER/BER derivation, we first elaborate how to calculate the LLRs and mutual information of RP-BICM-ID systems.

1) LLRs of RP-BICM-ID System: In the BICM-ID system, the LLRs for the global iterative decoding (i.e., iterative demapping and decoding) and those for the local iterative decoding (i.e., BP decoding) are defined as follows: $L_{\rm A,DEM}(j)$ is the *a-priori* LLR of $\widetilde{v}_j$ passing from the outer decoder to the inner demapper, $L_{\rm ch,DEC}(j)$ is the *equivalent initial channel* LLR of $\widetilde{v}_j$ passing from the inner demapper to the outer decoder, $L_{\rm E,DEM}(j)$ is the *extrinsic* LLR of $\widetilde{v}_j$ passing from the inner demapper to the outer decoder, $L_{\rm E,DEC}(j)$ is the *extrinsic* LLR of $\widetilde{v}_j$ passing from the outer decoder to the inner demapper, $L_{\rm APP,DEM}(j)$ is the *a-posteriori* LLR of $\widetilde{v}_j$ output from the inner demapper, $L_{\rm APP,DEC}(j)$ is the *a-posteriori* LLR of $\widetilde{v}_j$ output from the outer decoder, $L_{\rm Av}(i,j)$ is the *a-priori* LLR received by $\widetilde{v}_j$ on each edge connecting $\widetilde{v}_j$ to $\widetilde{c}_i$, $L_{\rm Ac}(i,j)$ is the *a-priori* LLR received by $\widetilde{c}_i$ on each edge connecting $\widetilde{c}_i$ to $\widetilde{v}_j$, $L_{\rm Ev}(i,j)$ is the *extrinsic* LLR passing from $\widetilde{v}_j$ to $\widetilde{c}_i$, $L_{\rm Ec}(i,j)$ is the *extrinsic* LLR passing from $\widetilde{c}_i$ to $\widetilde{v}_j$.

During the global iteration, the extrinsic LLRs output from the outer decoder are fed back to the inner demapper to serve as its a-priori LLRs. These LLRs can be utilized to improve the reliability of the a-posteriori LLRs of the output demapper. With the aid of the a-priori LLRs of the other $w-1$ bits, the

a-posteriori LLR of the μ-th bit b_{l_μ} within the l-th symbol x_l transmitted on α_l is calculated as

$$\begin{aligned} L_{\mathrm{APP,DEM}}(l_\mu) &= \ln \frac{\Pr(b_{l_\mu}=0|y_l)}{\Pr(b_{l_\mu}=1|y_l)} = \ln \frac{\sum_{x\in\chi_\mu^0} f(y_l|x_l=x)\Pr(x_l=x)}{\sum_{x\in\chi_\mu^1} f(y_l|x_l=x)\Pr(x_l=x)} \\ &= \ln \frac{\sum_{x\in\chi_\mu^0} f(y_l|x_l=x)\exp\left(\sum_{\mu'=1}^{w}(1-b_{l_{\mu'}})L_{\mathrm{A,DEM}}(l_{\mu'})\right)}{\sum_{x\in\chi_\mu^1} f(y_l|x_l=x)\exp\left(\sum_{\mu'=1}^{w}(1-b_{l_{\mu'}})L_{\mathrm{A,DEM}}(l_{\mu'})\right)}, \end{aligned} \tag{16}$$

where $b_{l_{\mu'}}$ is the μ'-th bit within the l-th symbol x_l, and $\mu' = 1,\ldots,\mu-1,\mu+1,\ldots,w$.

Without the employment of the a-priori LLRs of the other $w-1$ bits (i.e., $L_{\mathrm{A,DEM}}(l_{\mu'})=0$), the a-posteriori LLRs are calculated independently. Then, substituting (12) into (16) yields the a-posteriori LLRs output from the demapper in the RP-BICM-NI system, i.e.,

$$L_{\mathrm{APP,DEM}}(l_\mu) = \ln\left[\sum_{x\in\chi_\mu^0}\exp\left(-\frac{|y_l-x|^2}{2\left(\sigma_{n,l}^{(\mathrm{Eq})}\right)^2}\right)\right] \Bigg/ \left[\sum_{x\in\chi_\mu^1}\exp\left(-\frac{|y_l-x|^2}{2\left(\sigma_{n,l}^{(\mathrm{Eq})}\right)^2}\right)\right]. \tag{17}$$

2) Mutual Information of RP-BICM-ID System: Likewise, the mutual information for the RP-BICM-ID system can be defined as follows: $I_{\mathrm{A,DEM}}(j)$ is the *a-priori* MI between $\widetilde{v}_j$ and $L_{\mathrm{A,DEM}}(j)$, $I_{\mathrm{ch,DEC}}(j)$ is the *equivalent initial channel* mutual information between $\widetilde{v}_j$ and $L_{\mathrm{ch,DEC}}(j)$, $I_{\mathrm{E,DEM}}(j)$ is the *extrinsic* mutual information between $\widetilde{v}_j$ and $L_{\mathrm{E,DEM}}(j)$, $I_{\mathrm{E,DEC}}(j)$ is the *extrinsic* mutual information between $\widetilde{v}_j$ and $L_{\mathrm{E,DEC}}(j)$, $I_{\mathrm{APP,DEM}}(j)$ is the *a-posteriori* mutual information between $\widetilde{v}_j$ and $L_{\mathrm{APP,DEM}}(j)$, $I_{\mathrm{APP,DEC}}(j)$ is the *a-posteriori* mutual information between $\widetilde{v}_j$ and $L_{\mathrm{APP,DEC}}(j)$, $I_{\mathrm{Av}}(i,j)$ is the *a-priori* mutual information between $\widetilde{v}_j$ and $L_{\mathrm{Av}}(i,j)$, $I_{\mathrm{Ac}}(i,j)$ is the *a-priori* mutual information between $\widetilde{v}_j$ and $L_{\mathrm{Ac}}(i,j)$, $I_{\mathrm{Ev}}(i,j)$ is the *extrinsic* mutual information between $\widetilde{v}_j$ and $L_{\mathrm{Ev}}(i,j)$, $I_{\mathrm{Ec}}(i,j)$ is the *extrinsic* mutual information between $\widetilde{v}_j$ and $L_{\mathrm{Ec}}(i,j)$.

Based on the consistent-distribution assumption [38], [41], the mutual information between the input VN (i.e., coded bit) $\widetilde{v}_j$ and its corresponding output LLR $L(j)$ of a binary-input and continuous-output channel is expressed as

$$I(j) = 1 - \mathbb{E}\left[\log_2\left(1+\exp\left(-(-1)^{\widetilde{v}_j}L(j)\right)\right)\right], \tag{18}$$

where $\widetilde{v}_j \in \{0,1\}$. It has been proved in [18], [38] that (18) can also accurately estimate the mutual information even if the LLR distribution does not satisfy the consistency condition.

As a special case, if the output LLR of a channel follows a symmetric Gaussian, i.e., $L_{\mathrm{ch,DEC}} \sim \mathcal{N}(\sigma_{\mathrm{ch,DEC}}^2/2, \sigma_{\mathrm{ch,DEC}}^2)$, where $\sigma_{\mathrm{ch,DEC}}^2$ is the variance of $L_{\mathrm{ch,DEC}}$, one can readily get a simplified version of (18), i.e.,

$$I(\sigma_{\mathrm{ch,DEC}}) = J(\sigma_{\mathrm{ch,DEC}}) = 1 - \int_{-\infty}^{\infty}\frac{1}{\sqrt{2\pi\sigma_{\mathrm{ch,DEC}}^2}}\exp\left(-\frac{(\tau-\sigma_{\mathrm{ch,DEC}}^2/2)^2}{2\sigma_{\mathrm{ch,DEC}}^2}\right)\log_2\left[1+\exp(-\tau)\right]\mathrm{d}\tau. \tag{19}$$

This mutual information specifies the capacity of a BPSK-modulated AWGN channel. Furthermore, the inverse function of (19) is given by [20]

$$\sigma_{\mathrm{ch,DEC}} = J^{-1}(I) = \begin{cases} \beta_1 I^2 + \beta_2 I + \beta_3 \sqrt{I}, & 0 \leq I \leq 0.3646 \\ \beta_4 \ln[\beta_5(1-I)] + \beta_6 I, & 0.3646 < I \leq 1 \end{cases} \tag{20}$$

where $\beta_1 = 1.09542, \beta_2 = 0.214217, \beta_3 = 2.33727, \beta_4 = -0.706692, \beta_5 = 0.386013,$ and $\beta_6 = 1.75017$.

B. ML-PEXIT Algorithm for RP-BICM-ID Systems

As an asymptotic-performance analysis method, the EXIT function is of great usefulness to characterize the convergence behavior of the iterative detectors/decoders in channel-coded communication systems [41]. In particular, the conventional PEXIT algorithm for ergodic AWGN and fast-fading channels can be utilized to predict the decoding threshold and mutual information of a specific protograph code [42]. However, the outage region instead of the decoding threshold must be utilized to characterize the convergence performance of protograph codes over non-ergodic BF channels [11], [12]. In such channels, the outage-region and mutual-information metrics play an important role in the asymptotic WER and BER analysis. Unfortunately, the original PEXIT algorithm proposed for BF channels is based on the BPSK-signaling assumption [12], which is no longer effective for the scenarios with higher-order modulations and ID framework. To overcome this drawback, we develop an enhanced version of PEXIT algorithm so as to facilitate the performance analysis of RP-BICM-ID systems in BF scenarios. We refer to the enhanced PEXIT algorithm that takes both the larger complex-valued alphabets and iterative receiver into account as *ML-PEXIT algorithm*. It is because the newly proposed PEXIT algorithm can not only trace the extrinsic-mutual-information update at the node level (i.e., between VN and CN) within the BP decoder, but also trace the extrinsic-mutual-information update at the sub-decoder level (i.e., between the inner demapper and outer decoder) within the serial concatenated decoder.

Fig. 6 illustrates the block diagram of the ML-PEXIT algorithm. In the serial concatenated decoding scheme, one can easily observe the following properties: (i) in each global iteration, the extrinsic MI output from the demapper serves as the initial channel MI of the decoder, i.e., $I_{\mathrm{ch,DEC}}(j) = I_{\mathrm{E,DEM}}(j)$; the extrinsic MI output from the decoder serves as the a-priori LLR of the demapper, i.e., $I_{\mathrm{A,DEM}}(j) = I_{\mathrm{E,DEC}}(j)$, (ii) in the local iteration, the extrinsic MI output from the VN decoder serves as the a-priori MI of the CN decoder in each iteration, and vice versa, i.e., $I_{\mathrm{Ac}}(i,j) = I_{\mathrm{Ev}}(i,j)$ and $I_{\mathrm{Av}}(i,j) = I_{\mathrm{Ec}}(i,j)$. The above properties also hold in the LLR domain. Furthermore, in the proposed ML-PEXIT algorithm, the extrinsic MI output from the inner demapper is measured based on its a-priori MI and the channel information through the Monte-Carlo method, while the extrinsic MI output from the outer decoder is calculated based on its a-priori MI and the equivalent initial channel MI through information-theoretical derivation. After a sufficient number of iterations, the extrinsic MI output from the outer decoder converges to a saturated value. Utilizing the

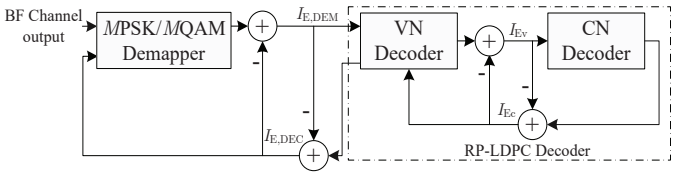

Fig. 6. Block diagram of the ML-PEXIT algorithm for the BICM-ID system over a BF channel.

above MI iterative procedure, one can calculate the a-posteriori MI of an RP-BICM-ID system and derive its corresponding outage region over BF channels.

Prior to the detailed algorithm description, we assume that: (i) an L-layer RP code and an MPSK/MQAM modulation are used, (ii) the maximum number of global iterations is $t_{\mathrm{GL,max}}$, and (iii) the maximum number of local iterations (BP iterations) is $t_{\mathrm{BP,max}}$. According to the above foundations, the proposed ML-PEXIT algorithm for the RP-BICM-ID system over a BF channel with L fading blocks can be described as below:

- **Initialization**

1) For $j = 1, 2, \ldots, n_{\mathrm{RP}}$, initialize the a-priori LLR of the demapper and channel LLR of decoder as $L_{\mathrm{A,DEM}}(j) = L_{\mathrm{ch,DEC}}(j) = 0$, and the current number of global iterations $t_{\mathrm{GL}} = 0$. For $l = 1, 2, \ldots, L$, initialize the received SNR $\gamma_{\mathrm{R},l}$ of the l-th fading block so as to obtain the SNR profile $\boldsymbol{\gamma}_{\mathrm{R}} = (\gamma_{\mathrm{R},1}, \gamma_{\mathrm{R},2}, \ldots, \gamma_{\mathrm{R},L})$ of the BF channel. Then, the noise variances of the L equivalent AWGN channels that correspond to the L fading blocks can be obtained using (9).
2) Randomly generate an M-ary symbol array of size $L \times N_s$, where the N_s symbols in the l-th ($l = 1, 2, \ldots, L$) row, denoted by $\{x_{l,1}, x_{l,2}, \ldots, x_{l,N_s}\}$, are transmitted in the l-th fading block of the BF channel. In particular, for $n_s = 1, 2, \ldots, N_s$, each symbol in the l-th fading block carries w ($w = L$) bits, i.e., $x_{l,n_s} \triangleq (b_{l_1}^{(n_s)}, b_{l_2}^{(n_s)}, \ldots, b_{l_w}^{(n_s)})$. The transfer PDFs of the l-th symbol row can be expressed as $\{f(y_l^{(1)}|x_l^{(1)}), f(y_l^{(2)}|x_l^{(2)}), \ldots, f(y_l^{(N_s)}|x_l^{(N_s)})\}$.

- **Calculation of Extrinsic Mutual Information Output from Demapper**

3) If $t_{\mathrm{GL}} = 0$, reset the current number of BP iterations to zero, i.e., $t_{\mathrm{BP}} = 0$. No a-priori LLR is fed back to the demapper (i.e., all a-priori LLRs equal 0). For $\mu = 1, 2, \ldots, w$, calculate the set of a-posteriori LLRs for the bit sequence $\{b_{l_\mu}^{(1)}, b_{l_\mu}^{(2)}, \ldots, b_{l_\mu}^{(N_s)}\}$ output from the demapper, i.e., $\{L_{\mathrm{APP,DEM}}^{(1)}(l_\mu), L_{\mathrm{APP,DEM}}^{(2)}(l_\mu), \ldots, L_{\mathrm{APP,DEM}}^{(N_s)}(l_\mu)\}$ by exploiting (17).
4) If $t_{\mathrm{GL}} > 0$, reset the current number of BP iterations to zero, i.e, $t_{\mathrm{BP}} = 0$. Based on the symmetric-Gaussian assumption in each fading block, estimate the standard deviation $\sigma_{L_{\mathrm{A,DEM}}(l_\mu)}$ of the a-priori LLRs of the demapper by substituting $I_{\mathrm{A,DEM}}(l_\mu)$ into (20). For $l = 1, 2, \ldots, L$ and $\mu = 1, 2, \ldots, w$, generate N_s LLR samples $\{\widehat{L}_{\mathrm{A,DEM}}^{(1)}(l_\mu), \widehat{L}_{\mathrm{A,DEM}}^{(2)}(l_\mu), \ldots, \widehat{L}_{\mathrm{A,DEM}}^{(N_s)}(l_\mu)\}$ for the μ-th bit within the l-th symbol output from the demapper, which follow the symmetric Gaussian distribution $N(\sigma^2_{L_{\mathrm{A,DEM}}(l_\mu)}/2, \sigma^2_{L_{\mathrm{A,DEM}}(l_\mu)})$. Afterwards, the a-priori LLR sequence $\{L_{\mathrm{A,DEM}}^{(1)}(l_\mu), L_{\mathrm{A,DEM}}^{(2)}(l_\mu), \ldots,$

$L_{\mathrm{A,DEM}}^{(N_s)}(l_\mu)\}$ corresponding to the bit sequence $\{b_{l_\mu}^{(1)}, b_{l_\mu}^{(2)}, \ldots, b_{l_\mu}^{(N_s)}\}$ can be measured by exploiting

$$L_{\mathrm{A,DEM}}^{(n_s)}(l_\mu) = (-1)^{b_{l_\mu}^{(n_s)}} \widehat{L}_{\mathrm{A,DEM}}^{(n_s)}(l_\mu), \quad n_s = 1, 2, \ldots, N_s. \tag{21}$$

Further, the a-posteriori sequence output from the demapper, i.e., $\{L_{\mathrm{APP,DEM}}^{(1)}(l_\mu), L_{\mathrm{APP,DEM}}^{(2)}(l_\mu), \ldots, L_{\mathrm{APP,DEM}}^{(N_s)}(l_\mu)\}$, can be calculated by substituting (12) and (21) into (16).

5) For $l = 1, 2, \ldots, L$ and $\mu = 1, 2, \ldots, w$, formulate the extrinsic LLR sequence output from the demapper, i.e., $\{L_{\mathrm{E,DEM}}^{(1)}(l_\mu), L_{\mathrm{E,DEM}}^{(2)}(l_\mu), \ldots, L_{\mathrm{E,DEM}}^{(N_s)}(l_\mu)\}$, by using

$$L_{\mathrm{E,DEM}}^{(n_s)}(l_\mu) = L_{\mathrm{APP,DEM}}^{(n_s)}(l_\mu) - L_{\mathrm{A,DEM}}^{(n_s)}(l_\mu), \quad n_s = 1, 2, \ldots, N_s. \tag{22}$$

6) For $l = 1, 2, \ldots, L$ and $\mu = 1, 2, \ldots, w$, estimate the extrinsic LLR of the μ-th bit b_{l_μ} within the l-th symbol x_l passing from the inner demapper to the outer decoder based on the ergodic theory and (18), i.e.,

$$I_{\mathrm{E,DEM}}(l_\mu) = 1 - \frac{1}{N_s} \sum_{n_s=1}^{N_s} \log_2 \left(1 + \exp\left(-(-1)^{b_{l_\mu}^{(n_s)}} L_{\mathrm{E,DEM}}^{(n_s)}(l_\mu)\right)\right). \tag{23}$$

- **Calculation of Extrinsic Mutual Information Output from Decoder**

7) If $t_{\mathrm{GL}} = t_{\mathrm{GL,max}}$ and $t_{\mathrm{BP}} = t_{\mathrm{BP,max}}$, stop the global iteration process and go to Step 16); else if $t_{\mathrm{GL}} < t_{\mathrm{GL,max}}$ and $t_{\mathrm{BP}} = t_{\mathrm{BP,max}}$, set $t_{\mathrm{GL}} = t_{\mathrm{GL}} + 1$, and go to Step 4); otherwise (i.e., $t_{\mathrm{GL}} \leq t_{\mathrm{GL,max}}$ and $t_{\mathrm{BP}} \neq t_{\mathrm{BP,max}}$), for $j = 1, 2, \ldots, n_{\mathrm{RP}}$, set the equivalent channel mutual information of the j-th VN $\widetilde{v}_j$ for the BP decoder as

$$I_{\mathrm{ch,DEC}}(j) = I_{\mathrm{E,DEM}}(j) = I_{\mathrm{E,DEM}}(l_\mu), \tag{24}$$

where $j = (l-1)L + \mu$ (i.e., the conversion from b_{l_μ} to $\widetilde{v}_j$).

8) For $i = 1, 2, \ldots, m_{\mathrm{RP}}$ and $j = 1, 2, \ldots, n_{\mathrm{RP}}$, if the number of edges connecting the j-th VN $\widetilde{v}_j$ to the i-th CN $\widetilde{c}_i$ is not equal to zero (i.e., $h_{i,j} \neq 0$), calculate the extrinsic MI passing from $\widetilde{v}_j$ to $\widetilde{c}_i$ by exploiting the equivalent channel mutual information, i.e.,

$$I_{\mathrm{Ev}}(i,j) = J\left(\sqrt{\left(\sum_{\xi \neq i} h_{\xi,j}[J^{-1}(I_{\mathrm{Av}}(\xi,j))]^2\right) + (h_{i,j}-1)[J^{-1}(I_{\mathrm{Av}}(i,j))]^2 + [J^{-1}(I_{\mathrm{ch,DEC}}(j))]^2}\right), \tag{25}$$

where $J(\cdot)$ is given in (19); otherwise (i.e, if $h_{i,j} = 0$), $I_{\mathrm{Ev}}(i,j) = 0$.

9) For $i = 1, 2, \ldots, m_{\mathrm{RP}}$ and $j = 1, 2, \ldots, n_{\mathrm{RP}}$, the a-priori mutual information received by $\widetilde{c}_i$ on each of the $h_{i,j}$ edges connecting $\widetilde{c}_i$ to $\widetilde{v}_j$ equals

$$I_{\mathrm{Ac}}(i,j) = I_{\mathrm{Ev}}(i,j).$$

10) For $i = 1, 2, \ldots, m_{\mathrm{RP}}$ and $j = 1, 2, \ldots, n_{\mathrm{RP}}$, if $h_{i,j} \neq 0$, the extrinsic mutual information passing from $\widetilde{c}_i$ to $\widetilde{v}_j$ is measured by

$$I_{\mathrm{Ec}}(i,j) = \left(1 - J\left(\sqrt{\left(\sum_{\xi \neq j} h_{i,\xi}[J^{-1}(1 - I_{\mathrm{Ac}}(i,\xi))]^2\right) + (h_{i,j}-1)[J^{-1}(1 - I_{\mathrm{Ac}}(i,j))]^2}\right)\right), \tag{26}$$

otherwise (i.e, if $h_{i,j}=0$), $I_{\mathrm{Ec}}(i,j)=0$.

11) For $i=1,2,\ldots,m_{\mathrm{RP}}$ and $j=1,2,\ldots,n_{\mathrm{RP}}$, the a-priori mutual information received by $\widetilde{v}_j$ on each of the $h_{i,j}$ edges connecting $\widetilde{v}_j$ to $\widetilde{c}_i$ equals

$$I_{\mathrm{Av}}(i,j)=I_{\mathrm{Ec}}(i,j).$$

12) For $j=1,2,\ldots,n_{\mathrm{RP}}$, calculate the extrinsic mutual information of $\widetilde{v}_j$ output from the decoder as (excluding the channel mutual information of the given VN)

$$I_{\mathrm{E,DEC}}(j)=J\left(\sqrt{\left(\sum_{\xi=1}^{m_{\mathrm{RP}}}h_{\xi,j}[J^{-1}(I_{\mathrm{Av}}(\xi,j))]^2\right)}\right). \tag{27}$$

13) The extrinsic mutual information $I_{\mathrm{E,DEC}}(j)$ will be fed back to the demapper in the next global iteration to serve as the a-priori mutual information of the μ-th bit b_{l_μ} within the l-th symbol x_l (transmitted on α_l). Thus, for $l=1,2,\ldots,L$ and $\mu=1,2,\ldots,w$, the a-priori mutual information of b_{l_μ} for the inner demapper equals

$$I_{\mathrm{A,DEM}}(l_\mu)=I_{\mathrm{A,DEM}}(j)=I_{\mathrm{E,DEC}}(j), \tag{28}$$

where $l=\lceil j/L\rceil$ and $\mu=j-(l-1)L$ (i.e., conversion from $\widetilde{v}_j$ to b_{l_μ}).

14) For $\widetilde{v}_j\in\mathcal{V}_{\mathrm{i}}$, calculate a-posteriori mutual information as

$$I_{\mathrm{APP,DEC}}(j)=J\left(\sqrt{\left(\sum_{\xi=1}^{n_{\mathrm{RP}}}h_{\xi,j}[J^{-1}(I_{\mathrm{Av}}(\xi,j))]^2\right)+[J^{-1}(I_{\mathrm{ch,DEC}}(j))]^2}\right). \tag{29}$$

15) If the a-posteriori mutual information values $I_{\mathrm{APP,DEC}}(j)=1$ for all information bits, i.e., $\forall\widetilde{v}_j\in\mathcal{V}_{\mathrm{i}}=\{\mathcal{V}_{\mathrm{i}1},\mathcal{V}_{\mathrm{i}2},\ldots,\mathcal{V}_{\mathrm{i}L}\}$, the iterative decoding is successful, stop the iterative process and go to Step 16); otherwise, set $t_{\mathrm{BP}}=t_{\mathrm{BP}}+1$ and go to Step 7) to continue the iteration process.

16) Repeat Step 2) to Step 15) for N_{A} different SNR profiles $\boldsymbol{\gamma}_{\mathrm{R}}^{(1)},\boldsymbol{\gamma}_{\mathrm{R}}^{(2)},\ldots,\boldsymbol{\gamma}_{\mathrm{R}}^{(N_{\mathrm{A}})}$ to yield the outage region for the RP code, i.e., $\overline{D}_{\mathrm{RP}}=\{\boldsymbol{\gamma}_{\mathrm{R}}\in\mathcal{R}_+^L\mid\exists\widetilde{v}_j\in\mathcal{V}_{\mathrm{i}}\text{ and }\exists\kappa>0,I_{\mathrm{APP,DEC}}(j)<1-\kappa\}$, in which the RP code cannot be successfully decoded. Similarly, the outage region for the j-th VN $\widetilde{v}_j$, which is defined as $\overline{D}_{\mathrm{RP},j}=\{\boldsymbol{\gamma}_{\mathrm{R}}\in\mathcal{R}_+^L\mid\exists\kappa>0,I_{\mathrm{APP,DEC}}(j)<1-\kappa\}$, can be also produced.

Remarks:

- The ML-PEXIT algorithm is a hybrid performance-analysis tool for RP-BICM systems and it intelligently incorporates Monte-Carlo simulation into information-theoretical derivation. To ensure the accuracy of the proposed ML-PEXIT algorithm (especially the calculation of extrinsic mutual information output from the inner demapper), the size of the M-ary symbol array (i.e., the number of symbol samples) $N'=L\times N_{\mathrm{s}}$ must be sufficiently large (i.e., $N_{\mathrm{s}}\geq 10^5$).

- When $t_{\mathrm{GL,max}} = 0$, the ML-PEXIT algorithm reduces to the simplest case because there is no global iteration. In this case, the algorithm can be used to calculate the outage region and mutual informaiton of RP-BICM-NI systems.
- Although we assume $q = 1$ in the ML-PEXIT algorithm, this algorithm can be applied to the cases of $q > 1$ by means of replacing the original protograph by an intermediate protograph.
- Unlike in a BPSK-modulated BF channel, in a BICM-BF channel, the L VNs in the same fading block may have different equivalent channel mutual information, which is attributed to the unequal demapping performance of the L component bits within an M-ary symbol. Consequently, the extrinsic mutual information of n_{RP} VNs output from the outer decoder should be independently fed back to the inner demapper so as to make a precise prediction of their convergence performance.
- Different from conventional protograph or LDPC codes, the information bits and parity bits in an RP code can be explicitly distinguished. In this sense, we only need to exploit the ML-PEXIT algorithm to estimate the convergence performance and error performance of information bits rather than the overall coded bits because their performance is determined by the former.
- The ML-PEXIT algorithm can be viewed as a further generalization of the PEXIT algorithm [12], since the high modulation and ID are taken into consideration in the former. More specifically, the proposed ML-PEXIT algorithm calculates the mutual information at two different levels, i.e., the node level and sub-decoder level. In particular, the ML-PEXIT algorithm contains many extra steps compared with that in [12], e.g., Steps 1) to 7) and Steps 13) to 14). In addition, as an ergodic AWGN channel evolves to a non-ergodic BF channel with L fading blocks, the outage region is expanded from a one-dimensional space to an L-dimension space.

C. Asymptotic WER and BER Expressions

According to [11], after t_{GL} global iterations, the conditional BER of a VN $\widetilde{v}_j$ under a fixed SNR profile $\boldsymbol{\gamma}_{\mathrm{R}} = (\gamma_{\mathrm{R},1}, \gamma_{\mathrm{R},2}, \ldots, \gamma_{\mathrm{R},L})$ can be evaluated using

$$P_{\mathrm{BER},j}^{t_{\mathrm{GL}}}(\boldsymbol{\gamma}_{\mathrm{R}}) = \frac{1}{2}\mathrm{erfc}\left(\frac{J^{-1}(I_{\mathrm{APP,DEC}}(j))}{2\sqrt{2}}\right), \tag{30}$$

where $\mathrm{erfc}(\cdot)$ represents the complementary error function. Note that $P_{\mathrm{BER},j}^{t_{\mathrm{GL}}}(\boldsymbol{\gamma}_{\mathrm{R}})$ is a non-increasing function of $I_{\mathrm{APP,DEC}}(j)$, and $P_{\mathrm{BER},j}^{t_{\mathrm{GL}}}(\boldsymbol{\gamma}_{\mathrm{R}})$ equals zero when $I_{\mathrm{APP,DEC}}(j) = 1$.

Moreover, as the L received SNRs $\gamma_{\mathrm{R},1}, \gamma_{\mathrm{R},2}, \ldots, \gamma_{\mathrm{R},L}$ are independent Gamma-distributed random variables, their joint PDF is given by

$$f(\boldsymbol{\gamma}_{\mathrm{R}}) = f(\gamma_{\mathrm{R},1}, \gamma_{\mathrm{R},2}, \ldots, \gamma_{\mathrm{R},L}) = f(\gamma_{\mathrm{R},1}) f(\gamma_{\mathrm{R},2}) \cdots f(\gamma_{\mathrm{R},L}). \tag{31}$$

In consequence, after t_{GL} global iterations, the asymptotic WER of an RP ensemble in the BICM-ID system over a BF channel with L fading blocks can be estimated by

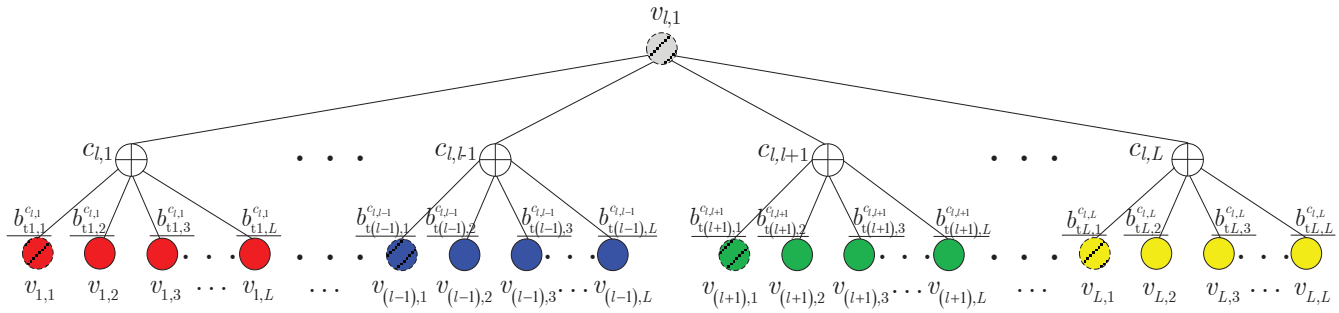

Fig. 7. Protograph of a type-l rootcheck set $\mathcal{C}_l = (c_{l,1}, \ldots, c_{l,l-1}, c_{l,l+1}, \ldots, c_{l,L})$ in a rate-$1/L$ L-layer RP code.

$$P_{\mathrm{W}}^{t_{\mathrm{GL}}} = \int \int \cdots \int_{\overline{D}_{\mathrm{RP}}} f(\gamma_{\mathrm{R},1}) f(\gamma_{\mathrm{R},2}) \cdots f(\gamma_{\mathrm{R},L}) d\gamma_{\mathrm{R},1} d\gamma_{\mathrm{R},2} \cdots d\gamma_{\mathrm{R},L}, \tag{32}$$

and the asymptotic BER can be estimated by

$$P_{\mathrm{B}}^{t_{\mathrm{GL}}} = \frac{L}{n_{\mathrm{RP}}} \sum_{\widetilde{v}_j \in \mathcal{V}_{\mathrm{i}}} \int \int \cdots \int_{\overline{D}_{\mathrm{RP},j}} P_{\mathrm{BER},j}^{t_{\mathrm{GL}}}(\boldsymbol{\gamma}_{\mathrm{R}}) f(\gamma_{\mathrm{R},1}) f(\gamma_{\mathrm{R},2}) \cdots f(\gamma_{\mathrm{R},L}) d\gamma_{\mathrm{R},1} d\gamma_{\mathrm{R},2} \cdots d\gamma_{\mathrm{R},L}. \tag{33}$$

Finally, the WER of an RP ensemble can be numerically calculated by substituting (3) into (32), while the BER of an RP ensemble can be numerically calculated by substituting (3) and (30) into (33).

V. UEP-Based Bit-to-Symbol Mapping Scheme for RP-BICM-ID Systems

As is well known, the w bits within each symbol for a given MPSK/MQAM constellation may possess different error performance, which indicate different levels of reliability [43]. Due to the above reason, the a-posteriori (or extrinsic) LLRs of these w bits output from the inner demapper of the RP-BICM-ID system may be different. As an example, for the anti-Gray-labeled 16QAM constellation (see Fig. 4(b)), the two bits b_{l_4} and b_{l_2} have relatively higher absolute LLR values than those of b_{l_3} and b_{l_1}. Hence, a UEP-B2S mapping scheme, which seamlessly combines the above property with the rootcheck structure, can be conceived to accelerate the convergence of BP iterative decoder in the RP-BICM-ID system. In this section, we commence the new mapping scheme by clarifying the structure of the rootchecks.

Example 3 – Type-l Rootcheck Set for an L-Layer RP Code. Assume a rate-$1/L$ L-layer RP code transmitted over a BF channel with L fading blocks. The protograph corresponding to this RP code must include L types of rootcheck sets so as to guarantee the full-diversity property. In particular, the protograph of a type-l rootcheck set $\mathcal{C}_l = (c_{l,1}, \ldots, c_{l,l-1}, c_{l,l+1}, \ldots, c_{l,L})$ is illustrated in Fig. 7. In this figure, $v_{l,1}$ $(l = 1, 2, \ldots, L)$ denotes the information-bit-related VN transmitted on α_l, $v_{l',\mu}$ denotes the μ-th $(l' = 1, \ldots, l-1, l+1, \ldots, L; \mu = 2, \ldots, L)$ parity-bit-related VN transmitted on $\alpha_{l'}$, $c_{l,l'}$ denotes the l'-th type-l rootcheck, and $b_{\mathrm{t}l',\mu'}^{c_{l,l'}}$ denotes the number of parallel edges connecting $c_{l,l'}$ to the μ'-th $(\mu' = 1, 2, \ldots, L)$ VN transmitted on $\alpha_{l'}$. As a result, the l'-th VN set transmitted on $\alpha_{l'}$ is given by $\mathcal{V}_{l'} = (\mathcal{V}_{\mathrm{i}l'}, \mathcal{V}_{\mathrm{p}l'}) = (v_{l',1}, v_{l',2}, \ldots, v_{l',L})$.

Suppose that the l-th $(l = 1, 2, \ldots, L)$ VN set of a regular L-layer RP code, i.e., $\mathcal{V}_l = (v_{l,1}, v_{l,2}, \ldots, v_{l,L})$, is mapped onto an M-ary symbol $x_l = (b_{l_1}, b_{l_2}, \ldots, b_{l_w})$ over a BF channel, where $w = \log_2 M = L$.

The mapping scheme between bit set $\mathcal{V}_l$ and symbol x_l is of particular importance to improve the overall performance of the BICM-ID system. Prior to the B2S mapping process, we re-rank the w bits within the M-ary symbol in a descending order of their demapping performance. The modified symbol is expressed as $x_l' = (b_{l_{\iota(1)}}, b_{l_{\iota(2)}}, \ldots, b_{l_{\iota(w)}})$, where $b_{l_{\iota(1)}}$ is the best-performing bit and $b_{l_{\iota(w)}}$ is the worst-performing bit. We consider two extremal schemes.

1) **Scheme I:** $v_{l,1}, v_{l,2}, v_{l,3}, \cdots, v_{l,L}$ are mapped onto $b_{l_{\iota(1)}}, b_{l_{\iota(2)}}, \ldots, b_{l_{\iota(w)}}$ in a sequential order, i.e., the information-bit-related VN $v_{l,1}$ in the l-th block is mapped onto the best-performing bit $b_{l_{\iota(1)}}$ in the M-ary symbol, while the $L-1$ parity-bit-related VNs are mapped onto the remaining $w-1$ bits in the symbol.
2) **Scheme II:** $v_{l,1}, v_{l,2}, v_{l,3}, \cdots, v_{l,L}$ are mapped onto $b_{l_{\iota(1)}}, b_{l_{\iota(2)}}, \ldots, b_{l_{\iota(w)}}$ in a reverse order, i.e., the information-bit-related VN $v_{l,1}$ in the l-th block is mapped onto the worst-performing bit $b_{l_{\iota(w)}}$ in the M-ary symbol, while the $L-1$ parity-bit-related VNs are mapped onto the remaining $w-1$ bits in the symbol.

Based on the re-ranking principle between x_l' and x_l, one can promptly obtain the mapping rule between $\mathcal{V}_l$ and x_l. For a given M-ary labeling that the w bits have unequal error probabilities (e.g., anti-Gray labeling), the RP-BICM-ID system with scheme II (referred to as *UEP-B2S mapping scheme*) must outperform that with scheme I over BF channels (from the information-bit perspective). It is because scheme II substantially exploits the UEP property of high-order modulation and rootcheck structure. In the following, we will propose a generalized proposition for this B2S mapping scheme and its proof.

Proposition 1. Consider an RP-BICM-ID system in a BF channel with L fading blocks, in which a regular L-layer RP code and MPSK/MQAM ($w = \log_2 M = L$) modulation are adopted. For the serial concatenated decoding framework, the BP decoder can achieve the best convergence performance if the information-bit-related VN in each fading block is mapped onto the component bit having the lowest-reliability in its corresponding symbol (i.e., if scheme II is adopted).

Proof. To simplify the exposition, we consider a block-erasure channel which is viewed as the extremal scenario of a BF channel (as in [2], [3]). Assume that the $L-1$ blocks (including the l-th block) are erased, i.e., $\alpha_1 = \ldots = \alpha_{l'-1} = \alpha_{l'+1} = \ldots = \alpha_L = 0$ and $\alpha_{l'} = +\infty$ ($l' \neq l$). Referring to Fig. 7, the recovery of the information bit $v_{l,1}$ in the l-th block is only dependent on the l'-th type-l rootcheck $c_{l,l'}$. In this sense, it is straightforward to observe which type of VNs in the l'-th block plays a more significant role in the recovery of $v_{l,1}$ under the BP iterative decoding. According to the construction method of regular RP codes (see Example 1*), the numbers of edges connecting the l'-th rootcheck $c_{l,l'}$ to its associated VNs must satisfy $b_{\mathrm{t}l',2}^{c_{l,l'}} = b_{\mathrm{t}l',3}^{c_{l,l'}} = \ldots, = b_{\mathrm{t}l',L-1}^{c_{l,l'}} = b_{\mathrm{p}l} = d_{\tilde{v}}/(L-1)$ and $b_{\mathrm{t}l',1}^{c_{l,l'}} = b_{\mathrm{i}l} = d_{\tilde{v}}/(2(L-1))$, where $d_{\tilde{v}}$ is the degree*

of VN. It means that $c_{l,l'}$ has $d_{\tilde{v}}/(L-1)$ edges connecting to each parity-bit-related VN transmitted on $\alpha_{l'}$ (i.e., there are in total $L-1$ parity-bit-related VNs in each block), but has only $d_{\tilde{v}}/(2(L-1))$ connecting to the information-bit-related VN transmitted on $\alpha_{l'}$ (i.e., there is only one information-bit-related VN in each block). Under the BP iterative decoding, the $L-1$ parity bits, i.e., $v_{l',2}, v_{l',3} \ldots, v_{l',L}$, transmitted on $\alpha_{l'}$ can feed much more extrinsic LLR to $v_{l,1}$ through the rootcheck $c_{l,l'}$ with respect to their corresponding information bit (i.e., $v_{l',1}$). Accordingly, the convergence performance of the information bit $v_{l,1}$ is mainly dependent on these $L-1$ parity bits rather than their corresponding information bit. The above conclusion also holds for a more general scenario, in which $L-L'$ $(1 < L' \leq L)$ blocks are erased. In consequence, the best convergence performance of a regular L-layer RP code can be guaranteed if the information-bit-related VN in each fading block is mapped to the lowest-reliable bit within its corresponding symbol. □

Remark: The principle of the proposed UEP-B2S mapping scheme is applicable to Gray-labeled MPSK/MQAM ($M \geq 8$) constellations and irregular RP codes. Nevertheless, we omit the extension because it is straightforward and trivial to the current work.

VI. Simulation Results and Discussions

Here, we present various error-rate simulation results of RP-BICM-ID systems with finite-length RP codes and MPSK/MQAM modulations over Nakagami-m BF channels. In particular, we focus on the rate-$1/2$ RP-2 code (two-layer RP code), the rate-$1/3$ RP-3 code (three-layer RP code), and the rate-$1/4$ RP-4 code (four-layer RP code) in the simulations (see *Example 1*).[4] We first compare the simulated and asymptotic error rates of the RP-BICM systems to demonstrate the accuracy of our theoretical analysis. Afterwards, we examine the error performance of the RP-BICM-ID systems in different scenarios to verify the merit of our design. Unless otherwise stated, we assume that the transmitted codeword length of all codes is $N_{\mathrm{RP}} = 1024$, the fading depth is $m = 1$, the number of fading blocks is $L = 2$, and the maximum numbers of global iterations and BP iterations are 5 and 50, respectively.

A. Comparison of Theoretical and Simulated Results

Fig. 8 plots the asymptotic and simulated WER curves of the RP-BICM systems over a BF channel, where a rate-$1/2$ RP-2 code is used. Especially, both asymptotic and simulated WERs are calculated based only on the correctness of the decoded information bits. It is apparent that the simulated WER curves are highly consistent with their corresponding asymptotic results regardless of the modulation order and labeling rule.[5]

[4]The derived graph (i.e, parity-check matrix) of an RP code can be constructed from its protograph (i.e., base matrix) by using the method in [14, Sect. IV-C].

[5]For BPSK modulation, it does not make sense to adopt iterative receiver for the system because each symbol only carries one bit.

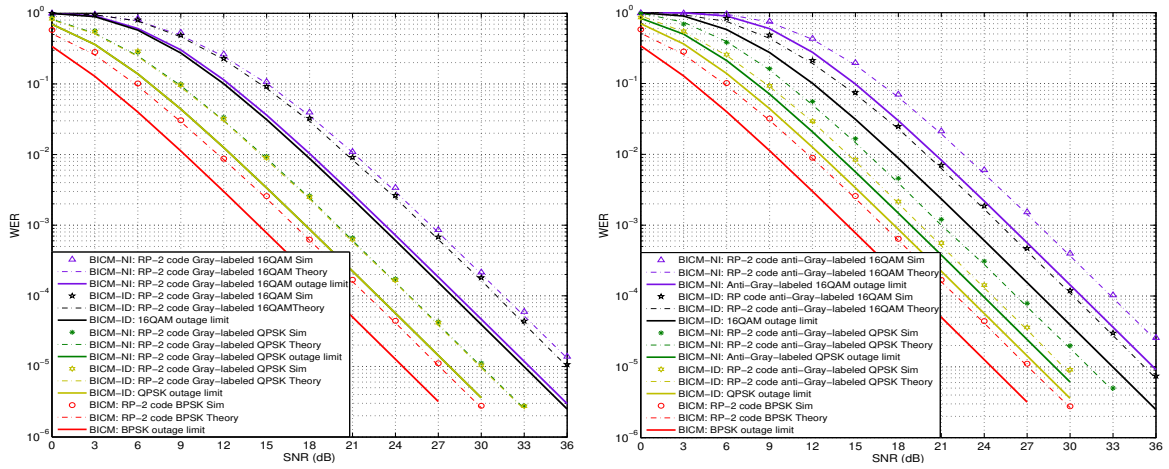

(a) (b)

Fig. 8. Theoretical and simulated WER results of the RP-BICM-ID/NI systems over a Nakagami BF channel: (a) Gray-labeling and (b) anti-Gray labeling. The parameters used are $r_{\mathrm{RP}} = 1/2, N_{\mathrm{RP}} = 1024, m = 1,$ and $L = 2$. Scheme I is adopted.

Moreover, we can observe that the proposed RP-BICM-ID/NI system has a WER slope identical to that of the outage limit, indicating the inherent full-diversity property. By comparing the curves in Fig. 8(a) and Fig. 8(b), we can also find that Gray labeling is superior to anti-Gray labeling in the RP-BICM-NI system, while the former is inferior to the latter in the ID scenario. In particular, Gray labeling only accomplishes trivial performance improvement utilizing ID, but anti-Gray labeling can achieve more than 2 dB gains utilizing ID. This observation agrees well with the conjecture in Sect. III. Besides, considering the 16QAM modulation, the anti-Gray-labeled RP-BICM-ID system has a gap of only 2 dB to the outage limit when $\mathrm{BER} = 10^{-5}$, while the Gray-labeled one has a gap of 3.2 dB to that limit. Simulations for different values of L and m have been performed to validate consistence between the theoretical and simulated results as well as the relative performance between the Gray and anti-Gray labelings over BF channels. In the following, we will restrict our attention to the anti-Gray labeling so as to illustrate the benefits of the RP-BICM-ID systems in a simple and clear way.

B. Comparison of Different B2S Mapping Schemes

As a further investigation, we compare the WER performance of the RP-BICM systems with two different B2S-mapping schemes. Referring to Fig. 9(b) on the 16QAM modulation, scheme II benefits from a performance gain of more than 0.6 dB compared with scheme I when $\mathrm{BER} = 2 \times 10^{-5}$ in both ID and NI scenarios.[6] Furthermore, exploiting scheme II, the RP-BICM-ID and RP-BICM-NI systems are only 1.5 dB and 2.0 dB away from their corresponding outage limits, respectively. Similar observations can be also made

[6]Simulations have been performed to show that scheme II also achieves a performance gain of about 0.6 dB over scheme I in both ID and NI scenarios under the Gray-labeled 16QAM modulation.

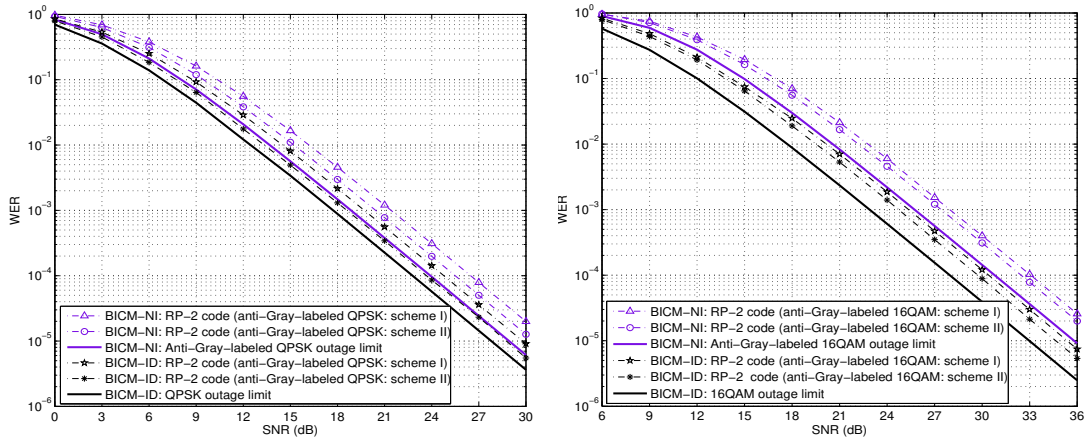

(a) (b)

Fig. 9. WER results of the RP-BICM-ID/NI systems with different B2S mapping schemes over a Nakagami BF channel: (a) QPSK and (b) 16QAM. The channel code used is the bilayer RP-2 code and the parameters used are $r_{\mathrm{RP}} = 1/2, N_{\mathrm{RP}} = 1024, m = 1,$ and $L = 2$.

for the results on QPSK modulation (see Fig. 9(a)). It is worth noting that a 1.5-dB gap to the outage limit over a BF channel is comparable to a 0.15-dB gap to the capacity limit over an AWGN channel because the SNR scale in the former is 10 times larger than that in the latter [2], [12]. Unless otherwise stated, we will only focus on the 16QAM-based BICM-ID systems with scheme II.

C. Comparison of RP Code and Conventional Protograph Codes

To substantially verify the superiority of the proposed RP-BICM-ID systems, we adopt the rate-$1/2$ regular $(3, 6)$ protograph code in [14], [39] and accumulate-repeat-by-4-jagged-accumulate (AR4JA) code in [12], [34] to implement the regular-protograph-BICM-ID and irregular-protograph-BICM-ID systems, and consider such two systems as benchmarks.[7] In Fig. 10(a), we show the WER performance of the proposed RP-BICM-ID system, regular-protograph-BICM-ID system and irregular-protograph-BICM-ID system over a BF channel. As can be seen, the RP-BICM-ID system significantly outperforms the regular-protograph-BICM-ID system, which further achieves an additional gain over the irregular-protograph-BICM-ID system. More importantly, only the RP-BICM-ID system exhibits full diversity and near-outage-limit performance. This phenomenon suggests that the regular protograph code constructed from a random parity-check matrix [34] and the irregular protograph code designed for ergodic channels [12], [34] no longer enjoy robustness against BF channels. In fact, all the state-of-the-art protograph and LDPC codes [28], [35], [36] proposed for ergodic BICM channels are not able to achieve full diversity in BICM-BF scenarios since their design methods do no take the non-ergodic property into account.

[7]The AR4JA code includes a type of punctured VNs, which is not transmitted through the channel [34]. Hence, such type of VNs is not considered in the calculation of codeword length.

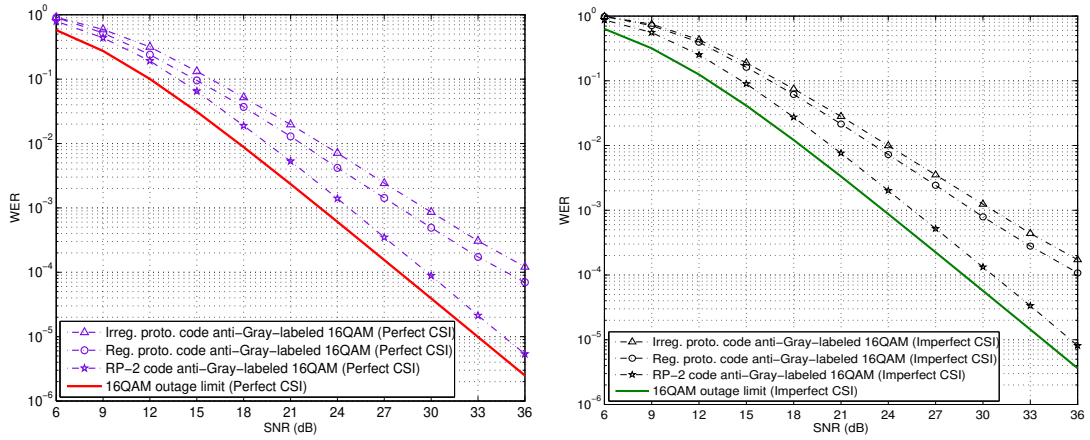

(a) (b)

Fig. 10. WER results of the proposed RP-BICM-ID system and two conventional protograph-BICM-ID systems over a Nakagami BF channel with (a) perfect CSI and (b) imperfect CSI. The parameters used are $r_{\rm RP} = 1/2, N_{\rm RP} = 1024, m = 1,$ and $L = 2$.

As a more practical setting, we study the error-correction capability of the RP-BICM-ID system over a Nakagami BF channel in the presence of imperfect CSI. According to [44], [45], with the use of a minimum-mean-square-error (MMSE) channel estimator, the estimated fading gain can be expressed as $\hat{\alpha}_l = \alpha_l + e_l$, where α_l is the actual fading gain, and e_l is the estimation error obeying the complex Gaussian distribution with zero mean and variance $\sigma_{\rm e}^2$ per dimension. We define the normalized estimation-error variance as the ratio of estimation-error variance to the scalar-fading-gain variance, denoted by $\eta_{\rm e} = \sigma_{\rm e}^2/\sigma_{|\alpha_l|}^2$, where $\sigma_{|\alpha_l|}^2$ is the variance of scalar fading gain $|\alpha_l|$. By setting $\eta_{\rm e} = 0.1$, Fig. 10(b) shows the WER results of the proposed RP-BICM-ID system and two conventional protograph-BICM-ID systems. As seen, the RP-BICM-ID system not only achieves full diversity (i.e., $d = 2$), but also significantly outperforms the other two counterparts in the imperfect-CSI scenario. Simulations have also been performed on different values of $\eta_{\rm e}$ (e.g., $\eta_{\rm e} = 0.15$) and similar results have been observed.

D. Discussion on Different Parameters

Fig. 11 shows the asymptotic and simulated WER/BER results of the RP-BICM-ID system with different codeword lengths over a BF channel. The results not only suggest that the asymptotic WER and BER expression can offer excellent estimates for finite-length RP codes, but also reveal that the error performance of RP-BICM-ID system is insensitive to the codeword length (or block length). Furthermore, the proposed system possesses the outage-limit-approaching feature irrespective of the codeword length. We also show the effect of the fading depth on the performance of RP-BICM-ID system over Nakagami BF channels in Fig. 12. It is clear that the proposed RP-BICM-ID system exhibits full-diversity performance (i.e., $d = mL$) for all the fading depths under study. Moreover, the system performance is substantially improved as the fading depth gradually reduces (i.e., as m gradually increases). Note that the proposed RP-BICM-ID-system

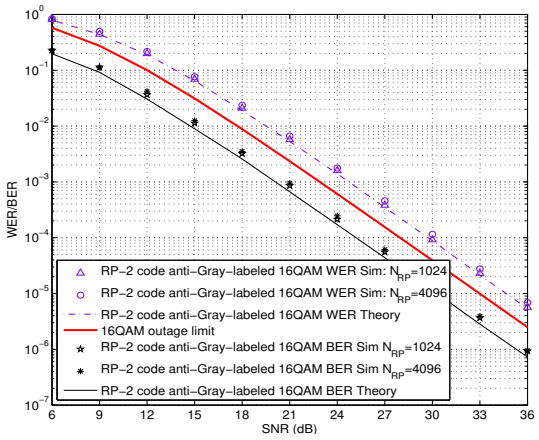

Fig. 11. BER and WER results of the RP-BICM-ID system with different codeword lengths over a Nakagami BF channel. The channel code used is the bilayer RP-2 code and the parameters used are $r_{\rm RP}=1/2, m=1, L=2,$ and $N_{\rm RP}=1024, 4096$.

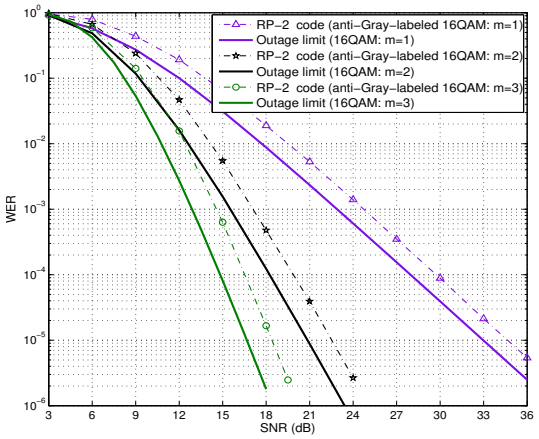

Fig. 12. WER results of the RP-BICM-ID system over Nakagami BF channels with different fading depths. The channel code used is the bilayer RP-2 code and the parameters used are $r_{\rm RP}=1/2, N_{\rm RP}=1024, L=2,$ and $m=1,2,3$.

design is not dependent on the fading distribution, and thus it is suited to other BF channel models, such as the Rician BF channel, without any change.

Finally, given a fixed spectral efficiency (i.e., $R_{\rm SE}=r_{\rm RP}w=1$), Fig. 13 presents the WER performance of three different RP-BICM-ID systems over Nakagmi BF channels. The codes, modulations, and number of fading blocks adopted by the three RP-BICM-ID systems are: i) rate-$1/2$ RP-2 code, QPSK and $L=2$, ii) rate-$1/3$ RP-3 code, 8PSK and $L=3$, and iii) rate-$1/4$ RP-4 code, 16QAM and $L=4$. On the one hand, all the three RP-BICM-ID systems possess WERs very close to their corresponding outage limits. On the other hand, the RP-4 code and RP-2 code enable the BICM-ID system to attain the best and worst error performance, respectively, due to their inherent diversity orders. Besides, the gap between the WER curve of the RP-BICM-ID system and the outage limit slightly increases with the increase of L (i.e., with the increase of modulation order). By properly incorporating irregularity into RP codes, irregular RP codes can be constructed to better match the modulation constellations. The irregular RP codes may not only preserve the full-diversity property, but also decrease the gap between the WER curve and the outage limit

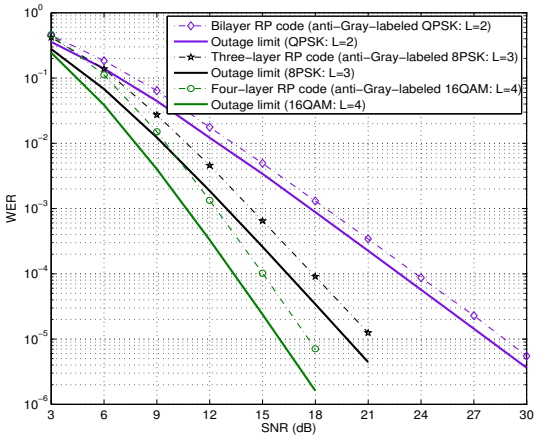

Fig. 13. WER results of three different RP-BICM-ID systems over Nakagami BF channels. The parameters used are $R_{\rm SE} = 1, N_{\rm RP} = 2880,$ and $m = 1$.

(especially in high-order modulation scenarios). However, the irregular RP codes suffer from more complex implementation compared with the regular RP codes. In actual implementation, the larger-layer (i.e., $L > 2$) RP codes (especially regular RP codes) are usually preferred with respect to the bilayer RP code because they are more likely to realize high-reliability and high-efficiency transmissions.

VII. Conclusions

In this paper, we have investigated the design and analysis of protograph codes in BICM-ID systems over non-ergodic BF channels. We have put forward a novel RP-BICM-ID system, which seamlessly combines the full-diversity RP codes and high-order modulations, to realize high-reliability and high-efficiency communication over such channels. We have also developed the outage-probability analysis and ML-PEXIT algorithm, which can be utilized to estimate the fundamental lower bounds and asymptotic error rates for the proposed RP-BICM-ID systems. We have discussed the effect of constellation labeling on the performance of RP-BICM-ID system and have found that anti-Gray labeling is superior to Gray labeling in BF scenarios. Additionally, based on the UEP property of both the RP codes and high-order modulations, we have conceived a new B2S mapping scheme for the RP-BICM-ID systems to further improve the error performance. Simulation results have demonstrated the tightness of our theoretical derivation and the merit of our system design. In particular, the RP-BICM-ID systems not only outperform the state-of-the-art counterparts but also achieve outage-limit-approaching WERs over BF channels. Thanks to the performance and efficiency advantages, the proposed RP-BICM-ID systems turn out to be a powerful transmission solution for slow-fading wireless communication applications.

References

[1] E. Biglieri, J. Proakis, and S. Shamai, "Fading channels: information-theoretic and communications aspects," *IEEE Trans. Inf. Theory*, vol. 44, no. 6, pp. 2619–2692, Oct. 1998.

[2] J. J. Boutros, A. G. i Fabregas, E. Biglieri, and G. Zemor, "Low-density parity-check codes for nonergodic block-fading channels," *IEEE Trans. Inf. Theory*, vol. 56, no. 9, pp. 4286–4300, Sep. 2010.

[3] D. Duyck, J. J. Boutros, and M. Moeneclaey, "Low-density graph codes for coded cooperation on slow fading relay channels," *IEEE Trans. Inf. Theory*, vol. 57, no. 7, pp. 4202–4218, Jul. 2011.

[4] D. Duyck, J. J. Boutros, and M. Moeneclaey, "Stability outage analysis for LDPC codes," *IEEE Commun. Lett.*, vol. 15, no. 11, pp. 1231–1233, Nov. 2011.

[5] M. Chiani, A. Conti, and V. Tralli, "Further results on convolutional code search for block-fading channels," *IEEE Trans. Inf. Theory*, vol. 50, no. 6, pp. 1312–1318, Jun. 2004.

[6] J. J. Boutros, A. G. i Fabregas, and E. C. Strinati, "Analysis of coding on non-ergodic block-fading channels," in *Proc. Allerton Conf. Commun., Control Comput.*, Sep. 2005, pp. 1–10.

[7] A. G. D. Uchoa, C. Healy, R. C. de Lamare, and R. D. Souza, "Design of LDPC codes based on progressive edge growth techniques for block fading channels," *IEEE Commun. Lett.*, vol. 15, no. 11, pp. 1221–1223, Nov. 2011.

[8] C. T. Healy and R. C. de Lamare, "Design of LDPC codes based on multipath EMD strategies for progressive edge growth," *IEEE Trans. Commun.*, vol. 64, no. 8, pp. 3208–3219, Aug. 2016.

[9] G. Lechner, K. D. Nguyen, A. Guillen i Fabregas, and L. K. Rasmussen, "Optimal power control for LDPC codes in block-fading channels," *IEEE Trans. Commun.*, vol. 59, no. 7, pp. 1759–1765, Jul. 2011.

[10] A. G. D. Uchoa, C. T. Healy, and R. C. de Lamare, "Iterative detection and decoding algorithms for MIMO systems in block-fading channels using LDPC codes," *IEEE Trans. Veh. Technol.*, vol. 65, no. 4, pp. 2735–2741, Apr. 2016.

[11] P. Pulini, G. Liva, and M. Chiani, "Unequal diversity LDPC codes for relay channels," *IEEE Trans. Wireless Commun.*, vol. 12, no. 11, pp. 5646–5655, Nov. 2013.

[12] Y. Fang, G. Bi, Y. L. Guan, and F. C. M. Lau, "A survey on protograph LDPC codes and their applications," *IEEE Commun. Surveys & Tutorials*, vol. 17, no. 4, pp. 1989–2016, 4th Quart. 2015.

[13] Y. Fang, G. Bi, and Y. L. Guan, "Design and analysis of root-protograph LDPC codes for non-ergodic block-fading channels," *IEEE Trans. Wireless Commun.*, vol. 14, no. 2, pp. 738–749, Feb. 2015.

[14] Y. Fang, S. C. Liew, and T. Wang, "Design of distributed protograph LDPC codes for multi-relay coded-cooperative networks," *IEEE Trans. Wireless Commun.*, vol. 16, no. 11, pp. 7235–7251, Nov. 2017.

[15] G. Caire, G. Taricco, and E. Biglieri, "Bit-interleaved coded modulation," *IEEE Trans. Inf. Theory*, vol. 44, no. 3, pp. 927–946, May 1998.

[16] X. Li, A. Chindapol, and J. A. Ritcey, "Bit-interleaved coded modulation with iterative decoding and 8PSK signaling," *IEEE Trans. Commun.*, vol. 50, no. 8, pp. 1250–1257, Aug. 2002.

[17] T. Cheng, K. Peng, Z. Liu, and Z. Yang, "Efficient receiver architecture for LDPC coded BICM-ID system," *IEEE Commun. Lett.*, vol. 19, no. 7, pp. 1089–1092, Jul. 2015.

[18] F. Schreckenbach, "Iterative decoding of bit-interleaved coded modulation," Ph.D. dissertation, Munich University of Technology, 2007.

[19] P. Chen, S. C. Liew, and L. Shi, "Bandwidth-efficient coded modulation schemes for physical-layer network coding with high-order modulations," *IEEE Trans. Commun.*, vol. 65, no. 1, pp. 147–160, Jan. 2017.

[20] S. ten Brink, G. Kramer, and A. Ashikhmin, "Design of low-density parity-check codes for modulation and detection," *IEEE Trans. Commun.*, vol. 52, no. 4, pp. 670–678, Apr. 2004.

[21] H. Zhou, M. Jiang, C. Zhao, and J. Wang, "Optimization of protograph-based LDPC coded BICM-ID for the Poisson PPM channel," *IEEE Commun. Lett.*, vol. 17, no. 12, pp. 2344–2347, Dec. 2013.

[22] I. Kang, H. Kim, and L. H. Hanzo, "EXIT-chart aided design of row-permutation assisted twin-interleaver BICM-ID," *IEEE Trans. Broadcast.*, vol. 64, no. 1, pp. 85–95, Mar. 2018.

[23] Z. Sun, L. Chen, X. Yuan, and Y. Yakufu, "Design and analysis of BICM-ID for two-way relay channels with physical-layer network coding," *IEEE Trans. Veh. Technol.*, vol. 66, no. 11, pp. 10 170–10 182, Nov. 2017.

[24] Q. Xie, K. Peng, J. Song, and Z. Yang, "Bit-interleaved LDPC-coded modulation with iterative demapping and decoding," in *Proc. IEEE Veh. Technol. Conf. (VTC)*, Apr. 2009, pp. 1–5.

[25] M. Franceschini, G. Ferrari, and R. Raheli, *LDPC Coded Modulations*. Berlin, Germany: Springer-Verlag, 2009.

[26] S. Che and S. Tong, "Low-complexity LDPC coded BICM-ID with orthogonal modulations," *Electronics Letters*, vol. 45, no. 16, pp. 845–846, Jul. 2009.

[27] J. Du, L. Yang, J. Yuan, L. Zhou, and X. He, "Bit mapping design for LDPC coded BICM schemes with multi-edge type EXIT chart," *IEEE Commun. Lett.*, vol. 21, no. 4, pp. 722–725, Apr. 2017.

[28] J. Hou, P. H. Siegel, L. B. Milstein, and H. D. Pfister, "Capacity-approaching bandwidth-efficient coded modulation schemes based on low-density parity-check codes," *IEEE Trans. Inf. Theory*, vol. 49, no. 9, pp. 2141–2155, Sept. 2003.

[29] F. Zabini, B. Matuz, G. Liva, E. Paolini, and M. Chiani, "The PPM poisson channel: Finite-length bounds and code design," in *Proc. Int. Symp. Turbo Codes & Iterative Inf. Process. (ISTC)*, Aug. 2014, pp. 193–197.

[30] R. Knopp and P. A. Humblet, "On coding for block fading channels," *IEEE Trans. Inf. Theory*, vol. 46, no. 1, pp. 189–205, Jan. 2000.

[31] Y. Li and M. Salehi, "A new BC-BICM scheme for block-fading channels," in *Proc. Annual Conf. Inf. Sci. Syst. (CISS)*, Mar. 2008, pp. 574–576.

[32] M. Elfituri, W. Hamouda, and A. Ghrayeb, "A convolutional-based distributed coded cooperation scheme for relay channels," *IEEE Trans. Veh. Technol.*, vol. 58, no. 2, pp. 655–669, Feb. 2009.

[33] A. Guillen i Fabregas and G. Caire, "Coded modulation in the block-fading channel: Coding theorems and code construction," *IEEE Trans. Inf. Theory*, vol. 52, no. 1, pp. 91–114, Jan. 2006.

[34] T. V. Nguyen, A. Nosratinia, and D. Divsalar, "Threshold of protograph-based LDPC coded BICM for Rayleigh fading," in *Proc. IEEE Glob. Telecommun. Conf. (GLOBECOM)*, Dec. 2011, pp. 1–5.

[35] Y. Jin, M. Jiang, and C. Zhao, "Optimized variable degree matched mapping for protograph LDPC coded modulation with 16QAM," in *Proc. Int. Symp. Turbo Codes & Iterative Inf. Process. (ISTC)*, Sept. 2010, pp. 161–165.

[36] Z. Liu, K. Peng, T. Cheng, and Z. Wang, "Irregular mapping and its application in bit-interleaved LDPC coded modulation with iterative demapping and decoding," *IEEE Trans. Broadcast.*, vol. 57, no. 3, pp. 707–712, Sept. 2011.

[37] J. Moualeu, W. Hamouda, H. Xu, and F. Takawira, "Multi-relay turbo-coded cooperative diversity networks over Nakagami-m fading channels," *IEEE Trans. Veh. Technol.*, vol. 62, no. 9, pp. 4458–4470, Nov. 2013.

[38] W. E. Ryan and S. Lin, *Channel Codes: Classical and Modern*. NewYork, NY, USA: Cambridge Univ. Press, 2009.

[39] D. Divsalar, S. Dolinar, C. Jones, and K. Andrews, "Capacity-approaching protograph codes," *IEEE J. Sel. Areas Commun.*, vol. 27, no. 6, pp. 876–888, Aug. 2009.

[40] S. ten Brink, J. Speidel, and R.-H. Yan, "Iterative demapping and decoding for multilevel modulation," in *Proc. IEEE Glob. Telecommun. Conf. (GLOBECOM)*, Nov. 1998, pp. 579–584.

[41] A. Ashikhmin, G. Kramer, and S. ten Brink, "Extrinsic information transfer functions: model and erasure channel properties," *IEEE Trans. Inf. Theory*, vol. 50, no. 11, pp. 2657–2673, Nov. 2004.

[42] G. Liva and M. Chiani, "Protograph LDPC codes design based on EXIT analysis," in *Proc. IEEE Glob. Telecommun. Conf. (GLOBECOM)*, Nov. 2007, pp. 3250–3254.

[43] N. Souto, R. Dinis, and J. C. Silva, "Analytical matched filter bound for M-QAM hierarchical constellations with diversity reception in multipath rayleigh fading channels," *IEEE Trans. Commun.*, vol. 58, no. 3, pp. 737–741, Mar. 2010.

[44] S. Hong, C. Seol, and K. Cheun, "Performance of soft decision decoded synchronous FHSS multiple access networks using MFSK modulation under Rayleigh fading," *IEEE Trans. Wireless Commun.*, vol. 59, no. 4, pp. 1066–1077, Apr. 2011.

[45] Z. Wang, D. Yang, and L. B. Milstein, "Multi-user resource allocation for a distributed multi-carrier DS-CDMA network," *IEEE Trans. Wireless Commun.*, vol. 60, no. 1, pp. 143–152, Jan. 2012.